VEHICLE ELECTRIFICATION USING AN

ELECTRIC AUXILIARY PLUG-IN DRIVE DEVICE

by Jonathan Serhal

A THESIS SUBMITTED TO THE FACULTY OF GRADUATE STUDIES

OF THE UNIVERSITY OF MANITOBA IN PARTIAL FULFILLMENT

OF THE REQUIREMENTS OF THE DEGREE OF

MASTER OF SCIENCE

Department of Mechanical Engineering

University of Manitoba

Winnipeg

Abstract

The majority of vehicles over the near term will rely on petroleum, with electric vehicles poised to take over a significant market share of new light duty vehicles in the near future. The introduction of new renewable electricity generation as a power source for these electric vehicles is highly desirable to solve energy drivers in transportation. The proposed Auxiliary Drive Device (ADD) instantly provides hybridization and electrification of an existing fossil fuel vehicle. It is a concept that may contribute to accelerate vehicle electrification. The ADD purpose is to contribute torque to increase fuel economy using mainly grid or regenerative electricity, and to compensate for the load born by a towing vehicle to reduce the engine size of that vehicle using mainly hybridization through the road concept.

The ADD is simulated, built and tested for the first time in a towing vehicle configuration. A test bench platform verifies controls on a push plate in a force sensor feedback control loop configuration. A sensor integrated mechanism is used to measure the force of the trailer load onto the towing vehicle. In addition, a scaled prototype provides experimental data to verify mathematical models developed for the ADD: an analytical static force model programmed in Excel. Torque contribution strategies provide acceleration to access performance and fuel economy gains. It is found that this new concept provides performance gains and fuel economy savings in a towing configuration. For the first prototype, the gains are relatively modest which is attributed to various frictional losses in the

first design iteration of the prototype. For the first prototype built, the ADD provides a 27.2% reduction in vehicle torque and 57.5% with the ADD and trailer combination. The system requires to be optimized to obtain further gains. It is recommended that the ADD single wheel approach be replaced with a dual wheel system to improve system performance when turning.

Acknowledgments

I would like to acknowledge funding from the NSERC strategic grant. I would also like to acknowledge and thank my advisor Dr. Eric Bibeau for his help and support in this project. As well to my parents and wife who encouraged me throughout this process where their support was an absolute staple.

Table of contents

List of symbols and abbreviations

ADD	auxiliary drive device
A_F	total vehicle frontal area
a_x	acceleration in the x-dir
C_D	coefficient of drag
cRIO	compact reconfigurable input/output module
C_{rr}	coefficient of rolling resistance
D_A	aerodynamic drag force
E_B	Baja belt clutch efficiency
E_C	Baja chain gear efficiency
E_D	Baja drive train efficiency
EM	electric motor
E_T	Total Baja overall drive train efficiency

FPGA	field programmable gate array integrated circuit
F_{VB}	vehicle braking force on ground
F_{VT}	vehicle torque force on ground
F_{XP}	x-dir. reaction force at push plate
F_{XT}	y-dir. reaction force at ADD hitch
F_{YP}	y-dir. reaction force at push plate
F_{YT}	X-dir. Reaction Force at ADD hitch
G	gravity constant
G_B	Baja chain gear ratio
GHG	green house gas
h_1	height of vehicle CoG
h_2	height of push plate
h_3	height of ADD CoG

h_4	height of ADD hitch
h_5	height of trailer CoG
h_A	height of consummate drag force
ICE	internal combustion engine
L_{PB}	length from push plate to ADD CoG
L_{PC}	length from PET CoG to ADD axle
L_{PT}	length from PET axle to ADD hitch
L_T	length from trailer CoG to axle
L_{TP}	length from hitch to trailer CoG
L_{Vf}	length of vehicle CoG to front axle
L_{VP}	length of vehicle rear axle to push plate
L_{Vr}	length of vehicle CoG to rear axle
NI	national instruments

PET	plug-in electrical trailer
PP	push plate force sensory device
R_{Xf}	front rolling resistance
R_{XP}	rolling resistance of ADD
R_{Xr}	rear rolling resistance
R_{XT}	trailer rolling resistance
SAE	Society of Automotive Engineer
SOC	State of Charge (for batteries)
T_P	PET torque force on ground
v	velocity of air/vehicle
W_P	total weight of ADD
W_{PA}	weight of ADD at axle
W_T	total weight of trailer

W_{TA}	weight of trailer at axle
W_V	total weight of vehicle
W_{Vf}	weight of vehicle at front axle
W_{Vr}	weight of vehicle at rear axle
ρ	air density

List of tables

List of figures

1 Introduction

1.1 Concept and Canadian vehicle usage

As of 2008, there were 19.4 million vehicles on the road in Canada, with an average of 293.6 billion kilometers driven and 31.3 billion liters of fuel consumed annually by light duty retail vehicles. According to Transport Canada, in 2008, 33% of Canadian energy use is in transportation. Of that 33%, 28% is used for on road vehicles. As far as GHG emissions are concerned, 27% come from transportation and 8.4% of that is for road vehicles. For domestic travel, 92% is by car, truck or recreational vehicles. On the road, for the last ten years, the car and van segments have surrendered 10% market share to larger fuel consuming vehicles like sport-utility and pickups truck models. Vans and sport-utility consume about 30% to 35% and trucks a staggering 50% more fuel in general compared to cars. Figure 1 shows the average fuel efficiency for car, van, sport-utility and pickup truck models from the period 2001 to 2008. We can see from Figure 2 that even though pickup trucks number on average 3.2 million and have 17.7% market share of the light vehicles on the road, they are driven on average 53.0 billion kilometers or 18.3% of total driven kilometers. Moreover, pickup trucks use an average 6.5 billion liters of fuel or 23.4% of the fuel consumed in Canada for light duty vehicles, as shown in Figure 3.

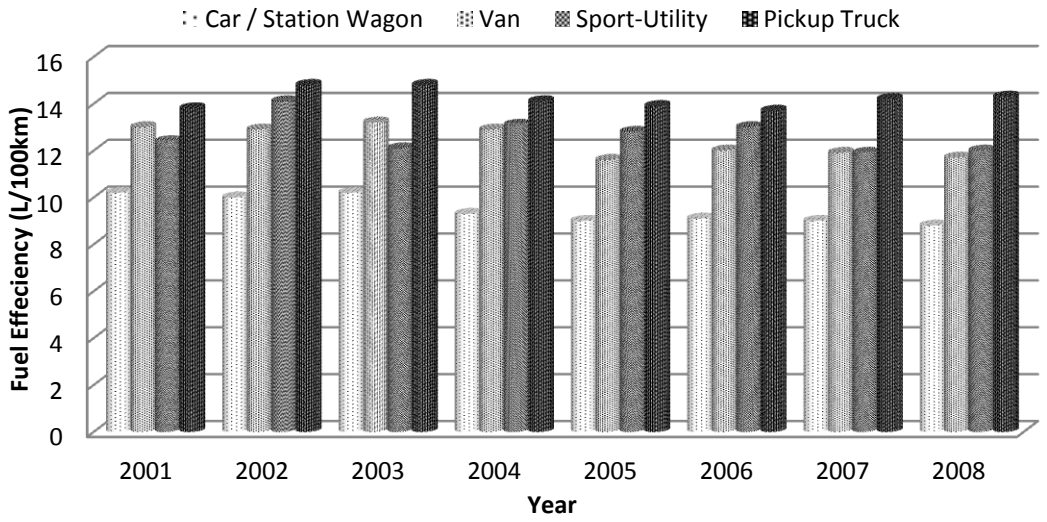

Figure 1: Fuel efficiency by vehicle type taken from Transport Canada reports on vehicle usage (L/100km) [1, 2, 3, 4, 5, 6, 7, 8, 9, 10]

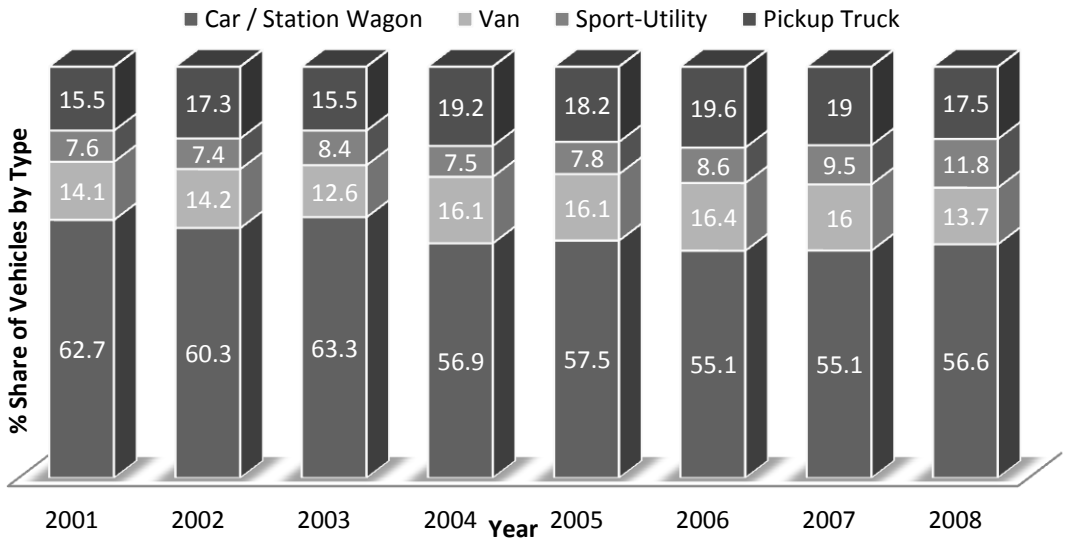

Figure 2: Percent share of vehicles by type from Transport Canada reports on vehicle usage [1, 2, 3, 4, 5, 6, 7, 8, 9, 10]

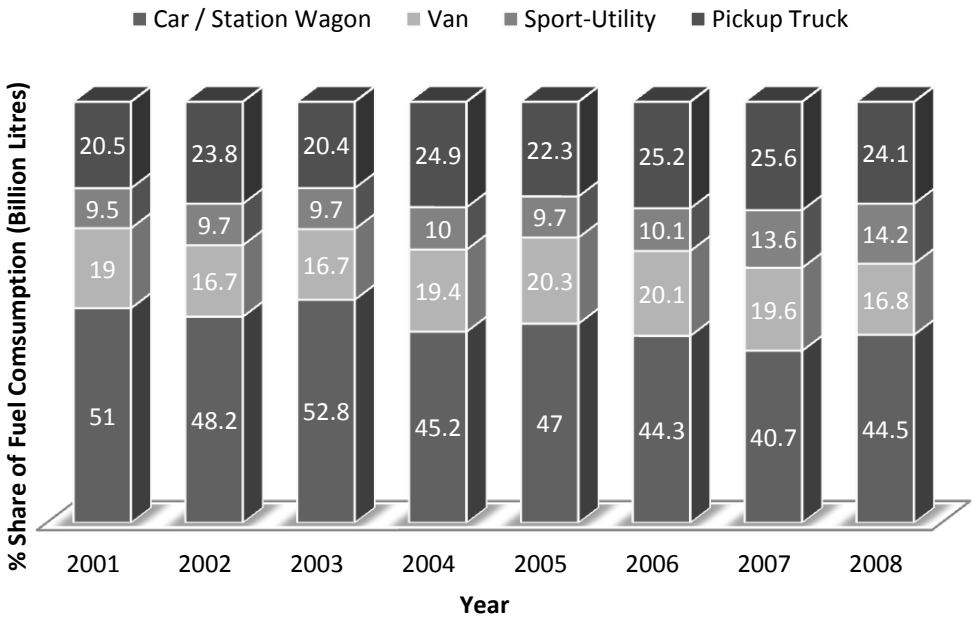

Figure 3: Billions of liters of fuel consumed annually of light duty vehicles in Canada from Stat Canada report on vehicle usage [1, 2, 3, 4, 5, 6, 7, 8, 9, 10]

This shows that trucks consume more fuel as a category even though they have a smaller market share proportionately. They consistently consume more than their market share.

1.2 The ADD concept to reduce vehicle emissions and fuel usage

New developments and vehicle technology can make a significant difference in energy consumption for road vehicles. However, one can ask if there is a simple retrofit device to permit electrification and hybridization of road vehicles like pickup trucks that operate exclusively on fossil fuels? Specifically, it would be advantageous if there was a

technology to reduce the emissions and fuel consumption of the largest contributors of GHG on the road that is easily to implement. Various methods already exist to electrify vehicles. None are simple. For example, it is possible to remove wheel hubs and replace them with electric motor wheel hubs, and hybrid vehicles like the Prius can be converted to a plug-in hybrid by adding a new battery pack in less than 4 hours.

A simple method is introduced by Reza Ghorbani and Dr. Eric Bibeau to convert any vehicle into a relatively low efficiency hybrid, plug-in hybrid and electric vehicle in less than 1 minute but limited to various operational constraints. They proposed and developed the Auxiliary Drive Device (ADD) shown in Figure 4 to accelerate the electrification of road vehicles. The ADD was originally developed to improve the emissions of pickup trucks that tow an occasional load with a trailer. It is a device that can save on emissions and fuel. ADD however is applicable to any road vehicle that can accept a hitch.

The ADD is connected to a vehicle through a hitch, and then autonomously endeavours to contribute thrust and braking forces seamlessly, like a hybrid motor that is integrated in an existing vehicle, but detachable at any time. As mentioned, the original concept was for a vehicle that tows a trailer to act as an intermediary device between the towing vehicle and the trailer where the controller compensates for a trailer to the point of zero force on the towing vehicle.

The potential largest contribution of ADD to reduce fuel consumption is to provide additional torque when a vehicle tows a load to entice consumers to buy trucks with smaller engines. It was postulated that consumers occasionally require a larger engine to tow a load. In this duty cycle, the full engine power is only used occasionally. ADD provides torque to tow a load to decrease the requirements and need to buy larger pick-up trucks by using a hybrid through the road strategy: use regenerative breaking to store power onboard the ADD to provide the towing vehicle occasional torque when required when passing or going up an incline.

However, the ADD is able to have several modes and functions for all vehicles. It can contribute by adding acceleration and braking to vehicles, can aid in passing on the highway, can be used to save fuel by providing toque when the engine is operating at low efficiency at low speed, can displace fossil fuel with grid power through plug-in of it on-board battery, can provide auxiliary power when not in use, and can use regenerative braking.

Acceleration produces the worst emissions for fuel burning vehicles and the ADD can provide electrical traction during that phase. During the acceleration phase, low air/fuel ratios results in improper burning leading to un-burnt fuel and temperature spikes which leads to higher carbon, nitrogen and sulfur based molecules in exhaustion which are the main contaminants of fuel burning engines. The ADD attempts to effectively reduce these emissions during that phase of vehicle use.

The ADD controller has various possible configuration modes include idling mode, hybrid only mode, hybrid though the road mode, plug-in mode, pure electric mode, charge depletion mode, trailer mode and auxiliary power unit mode. This thesis is focused on the ADD as configured when towing a load to reduce the engine size for pickup trucks. Other operational modes are not addressed.

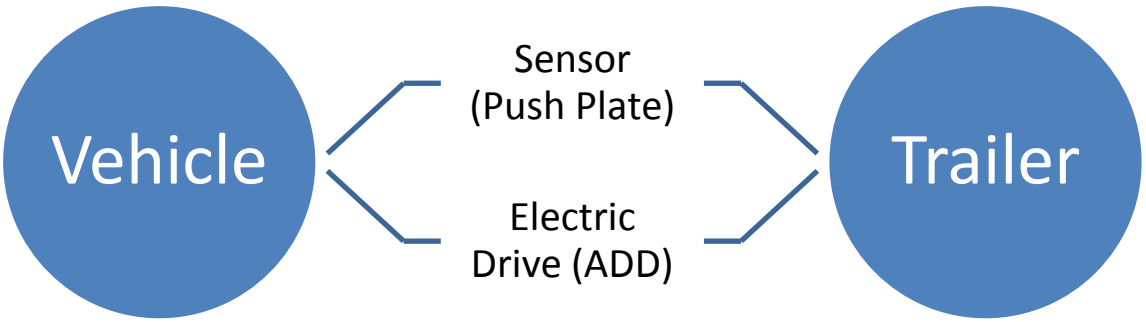

Figure 4: The ADD concept as introduced in this thesis to electrify the power train of existing fossil fuel vehicles to accelerate the electrification of road vehicles worldwide

1.3 Hybrid powertrains

To understand how ADD achieves electrification of an ICE engine vehicle, it is best to first review the type of hybridization and electrification of existing vehicles. In general, hybrization refers to the coalescing of two separate entities for a common goal. "Hybrid" more recently has been popularly used to describe a hybrid vehicle which uses electric power to supplement the power of an ICE, whether for performance, efficiency or both.

As emissions and fuel efficiency are contemporarily more important than performance and horsepower typically the electric power is used as fuel subsidization.

Electric motors (EM) are able to provide torque from virtually zero rotation as can be seen in rotary actuators or servomotors that allow for precise control of angular position, velocity and acceleration [11, 12]. EM's inherently are able to provide efficient torque without optimal rotation speeds when compared to ICE's. This is one of major advantages a hybrid power system has over a pure ICE. The coupling of the electric power delivery can be designed to deliver power at less optimal times for the ICE significantly reducing fuel consumption and emissions at opportune times. The three most common available types in the motor vehicle industry are the series, parallel, or series-parallel otherwise known as the power-split.

1.3.1 Series hybrids

The simplest ICE-EM configuration is in series where the EM is directly responsible for all wheel torque. Typically the EM is powered by a battery pack or a generator converting power from an ICE to electric stored in the batteries or regenerative braking. Regenerative braking is from extracting current from the EM thus creating a resistance to torque providing a braking force, in addition to a mechanical braking force from disk or drum brakes. Regenerative braking is only about 10% effective and still often requires mechanical brakes for full braking force and is difficult in practice because batteries in

general accept low amounts of current, but can deliver much larger amounts of current. Energy can be gleaned through regeneration depositing charge and increasing overall power consumption efficiency. Power storage is provided by a battery pack from either plugging it in or from a generator charge. The charge maintenance and delivery is governed by strategic computer admittance. The battery pack in series hybrids is much larger than parallel hybrid systems because peak power demand is not provided directly by the ICE (see Parallel hybrids for more information).

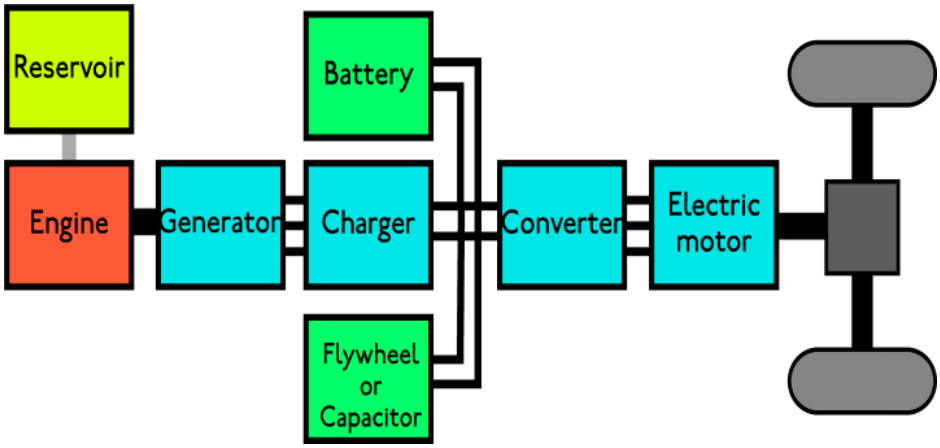

Figure 5: Series hybrid system diagram as in the Chevrolet Volt [13]

Conventional operating conditions of the ICE is during the inefficient power delivery periods of the engine thus providing the advantage of an EM. The ICE in a series configuration is directly coupled to wheel torque forcing it to perform under its inefficient range. In a series configuration it is decoupled and then is able operate at peak

efficiency and power delivery to run the generator. These systems are better at city stop and go driving versus highway efficiency.

1.3.2 Parallel hybrids

Contemporarily, the most common type of hybrid vehicle systems are in a parallel configuration. In parallel, two power sources joined to a single axle must necessarily have matching rotational speed in order for both torque contributions to combine. Here the ICE and EM are coupled through differential gearing. If there is no differential gearing each power source can only contribute torque individually and thus require to be disengaged from the drive axle through a mechanism such as a clutch or freewheel. An electric bicycle is an example of this. A simplistic solution of using a differential gearing with a fixed ratio and each source clutched. This allows for strategic torque input from either power source.

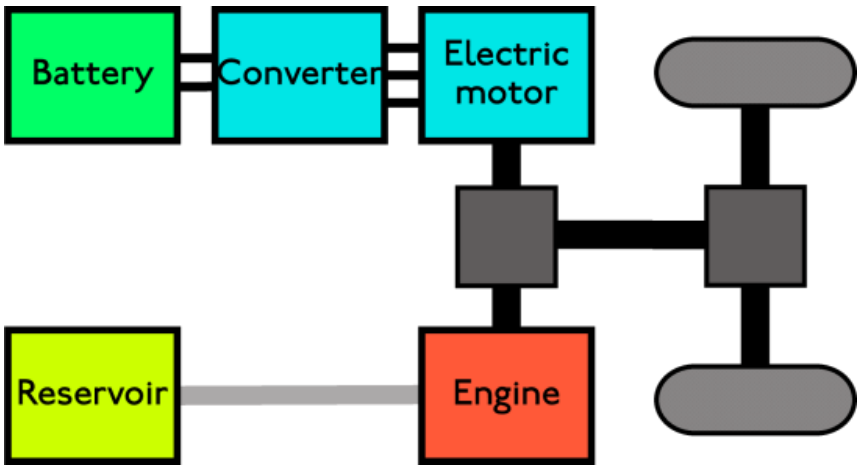

Figure 6: Parallel hybrid system diagram as in the Honda Insight [14]

Another form of parallel hybrid assumes constant invariable traction between front and rear axles while contacting road. Each axle is typically powered by its own source, one from an ICE and the other from an EM system. Regenerative braking can be implemented by loading the electric driven axle while the vehicle is being propelled by the ICE axle. Typically these systems rely more on regenerative braking and have smaller battery packs. Their performance is more efficient in highway driving versus city, stop and go, driving. Thus the parallel system is limited through traction of the contact to the road surface. This method has flexibility when portioning torque with the parallel power sources contributions on separate axles, but requires contingency when a loss of traction occurs on an individual axle.

1.3.3 Series-parallel hybrid

The series-parallel hybrid system uses an electric motor to drive the vehicle at low loads and low speeds and the gasoline engine when loads and speeds increase. The electric motor and the gasoline engine can work individually, or together, depending on the power required to drive the vehicle. In addition, as the system drives the wheels, the combustion engine drives a generator to simultaneously generate electricity to recharge the battery when necessary.

A control unit determines the best balance of engine and electric power to achieve the most efficient vehicle operation. The combustion engine operates within its most efficient range resulting in a vehicle that reduces exhaust emissions by 80% to 90% compared to conventional vehicles. It also produces about half the amount of carbon dioxide. The electric motor uses power from a high voltage battery, which is charged by the internal combustion engine, and by reclaiming the waste energy of decelerating or braking.

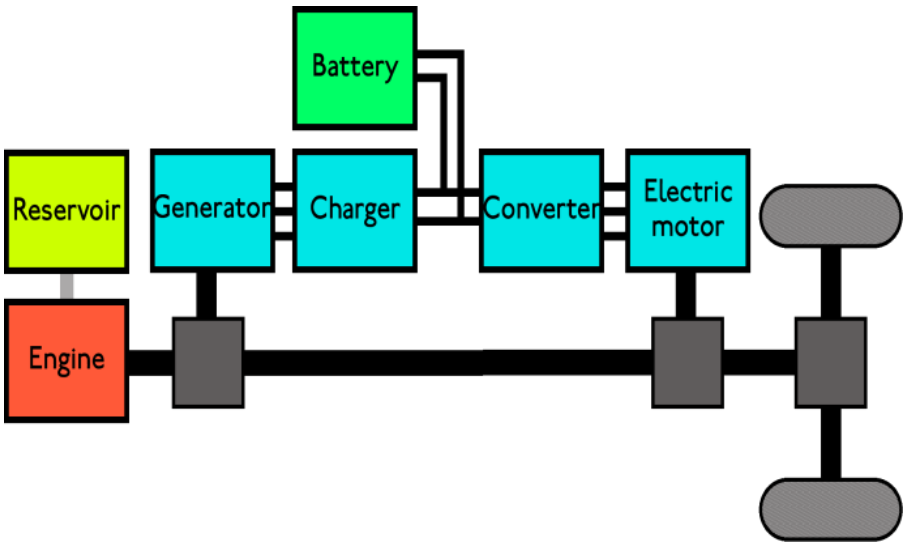

Figure 7: Series-parallel hybrid system diagram as in the Toyota Prius PHEV [15]

1.3.4 DC/DC controllers

As part of electric vehicles, motor controllers are an important element. To better understand the ADD system and how controllers are implemented, these are now discussed. Motor controllers are devices, or typically a group of devices, used to govern an electric motor by manipulating its input power. In general, electric motors are passive and require appropriate active control to function. Motor controllers may have a variety of features depending on application and type of motor.

In the simplest the case, the active control may be a basic switch and/or relay connecting and disconnecting the full supply of power to the electric motor allowing the motor to run at a single speed. Multi-purpose switches may also control multiple speeds, reversing

direction and voltage control for start-up. Over current and overload protection is typically required and provided by the supply circuit. For smaller motors built-in automatic circuits open to prevent overload. In larger motors overload relays with shunts and fuses or circuit breakers maintain the required protection. Automatic motor controllers sometimes use limit switches and other circuits to add protection.

More complex motor controllers may be used to accurately control the speed and torque of the connected motor (or motors) and may be part of closed loop control systems for precise positioning of a driven machine. For example, a numerically controlled lathe will accurately position the cutting tool according to a pre-programmed profile and compensate for varying load conditions and perturbing forces to maintain tool position.

Motor controllers can be manually, remotely or automatically operated. They may include only the means for starting and stopping the motor or they may include other functions [16]. An electric motor controller can be classified by the type of motor it is to drive such as permanent magnet, servo, series, separately excited, and alternating current.

1.4 Research objectives and proposed methodology

The objective of this work is to verify the potential of the proposed ADD system to contribute to fuel and GHG reductions using a simple and rapid conversion of a vehicle with a hitch using electrification of the powertrain.

To achieve this objective, it is proposed to focus exclusively on a vehicle in tow mode. Moreover, the methodology is composed of three steps:

1. Develop a 1-D analytical model of the ADD system in tow mode
2. Develop a test bench to develop a push plate and test a control strategy when towing a vehicle with an ADD
3. Build and test the first ADD prototype towing a load and gather experimental data to quantify performance, implementing the controller developed using the test bench facility.

2 Literary review

As ADD is a novel concept so the literature review is focused on contributions in the field of vehicle electrification for which the ADD design process relied upon to achieve an optimized configuration for the hardware and control system.

2.1 Torque control strategy for a parallel hydraulic hybrid vehicle

Hui Sun [17], in his paper showed that vehicle hybrid systems can utilize hydraulic power as an addition or supplementation to vehicle power source because of their high power density which accepts a high rate and frequency of torque charging and discharging making it ideal for off-road and heavy duty trucks. A Parallel Hydraulic Hybrid Vehicle (PHHV) can improve engine working efficiency through braking energy regeneration. The simulation employed a fuzzy logic control strategy for the torque and energy management. The hydraulic system used a reversible pump/motor for absorbing/applying torque and an accumulator to store the energy. The vehicle load changes will be offset by the control strategy through the torque dispersion between power sources. It was shown to be a practical and feasible method for improving fuel economy.

2.2 Control strategy and simulation analysis of a hybrid electric vehicle

Hybrid electric vehicle design involves sophisticated control strategies for power source management. Optimization is key in development of concepts and different design configurations. Zhao Shupeng et al. [18] analyzed three hybrid configurations, Series Hybrid Electric Vehicle (SHEV), Parallel Hybrid Electric Vehicle (PHEV), and Parallel-Series Hybrid Electric Vehicle (PSHEV). They simulated each power train using three different control strategies, Electric Assist Control (EAC), Adaptive Control Strategy (ACS), and Genetic Algorithms Control (GAC), with two different driving cycles, European city and road driving cycle, CYC_NEDC, and USA highway driving cycle, CYC_HWFET.

SHEV is a high efficiency and low exhaust emissions system that does well in complex or city driving. Advantages are that vehicle load doesn't directly affect efficiency and emissions as well as the ability maintain the ICE in its optimal efficiency range. PHEV is better for simple or highway driving conditions, gains overall better fuel consumption and can be managed easily at high efficiency. PSHEV in this case is a clutch system between a series and a parallel configuration. For control the SHEV will be engaged for the city driving and the PHEV for the highway driving. This way the best characteristics of each configuration can be applied. There is better transmission efficiency, fuel consumption with less harmful emission; however, costs are higher because of the complexity and number of components.

EAC manages the main power, the battery State of Charge (SOC) and the EM. In this case, when the ICE is under low efficiency and speed the EM will provide all of the drive torque. When the ICE is at high efficiency and speed the EM will on provide marginal or additional driving torque. This condition also assumes a certain level of charge can be taken from the ICE when the SOC is low and regenerative braking is possible.

ACS is real-time control based on minimizing fuel consumption and exhaust emissions for a range of torque applications. It is also optimized for maintaining SOC and efficient application EM torque. However, there are limitations in this approach because fuel consumption and emissions aren't the best indicators in efficient engine control and aren't optimized at a particular point, but rather a region with compromises.

GAC manages SOC, regenerative braking and engine temperature based on driving cost. A least object function on the engine and EM was used with floating point coding and a cross probability of 0.95 and aberrance of 0.05. The arithmetic operators are selected by the proportional method, resulting in different generations for torque and speed, but converged for an optimized 20^{th} generations satisfying all required criteria. The least object function used is:

$$f(x) = \begin{cases} c_{max} - g(x), & g(x) < c_{max} \\ 0, & other \end{cases} \quad 2.2\text{-}1$$

The simulation was done in ADVISOR2002 using the CYC_NEDC, which is a 1200 second sample with an average speed of 32.5 km/h and the CYC_HWFET, which is a 800 second sample with an average speed of 77.6 km/h. The vehicle weighed 1350 kg and a coefficient of drag at 0.335. The engine or power source was a 1.0 L, 41 kW ICE with a 75 kW EM with a 12 V, 26 Ah lead battery. The results are shown in Table 1.

Table 1: ADVISOR2002 simulation results from a hybrid electric vehicle showing the improvement on fuel economy and reduction in emissions by different control strategies

Control Strategy	**Driving Cycle**	**Fuel Economy** (L/100km)	**HC** (g/km)	**CO** (g/km)	**NOx** (g/km)
EAC	CYC_NEDC	5.9	0.343	1.472	0.255
	CYC_HWFET	4.7	0.253	1.18	0.207
ACS	CYC_NEDC	4.6	0.283	2.51	0.22
	CYC_HWFET	4.1	0.231	1.596	0.2
GAC	CYC_NEDC	3.4	0.285	1.341	0.203

Table 1 shows that ACS improved on the EAC strategy in both the driving cycles, CYC_NEDC and CYC_HWFET. Additionally, GAC for the only driving cycle simulated, CYC_NEDC, dramatically improved even further on fuel economy and emissions except for the relatively comparable HC emissions with ACS. The

improvement GAC created was almost the best results overall with the CYC_NEDC even though it is more demanding than the CYC_HWFET. These results are significant as they show the strong influence of a control strategy for a hybrid electric vehicle on the fuel consumption and harmful emissions exhausted by ICE engines. A similar result is expected for ADD implementation.

2.3 Hybrid electric vehicle control strategy based on power loss calculations

Steven Boyd in a paper [19]about entering a hybrid vehicle into the Challenge X competition wrote how a 2005 Chevrolet Equinox is electrically hybridized and analyzed. The Challenge X is a student design competition aimed at advancing vehicle technology, specifically cross-over's and SUV's. The overall evaluation is generally based well-to-wheel consumption, more particularly including petroleum consumption, fuel economy, decreasing emissions while maintaining performance, consumer appeal and safety. Results from this paper were studied when developing the ADD hardware and software for the controller.

In that competition, it was decided to modify a 2005 Chevrolet Equinox E85 and to use Power-Train System Analysis Toolkit (PSAT) software to evaluate the component implementation and overall vehicle performance simulation. Electrifying the rear axle of the vehicle satisfied the All-Wheel Drive (AWD) requirement of the competition, improving on a "through the road" system by having a more flexible power split engine

and motor with a direct "series" path to the battery charge control. It was determined that the best approach for the competition would be a Split Parallel Architecture (SPA) with a Belted Alternator Starter (BAS) and a Rear Traction Motor (RTM) to electrically torque the rear axle. Functionally this means a BAS, a small electric motor/generator, is connected to the ICE through a belt enabling it to both supplement torque demand and siphon torque for charging the batteries for the RTM connected to the rear axle. A belt drive allows for a lighter high speed motor coupled with a ratio speed reduction to simplify mechanical integration compared to the integration of an engine flywheel. A diagram of the system can be seen in Figure 8. This development influenced the decision to use a belt in the first ADD design.

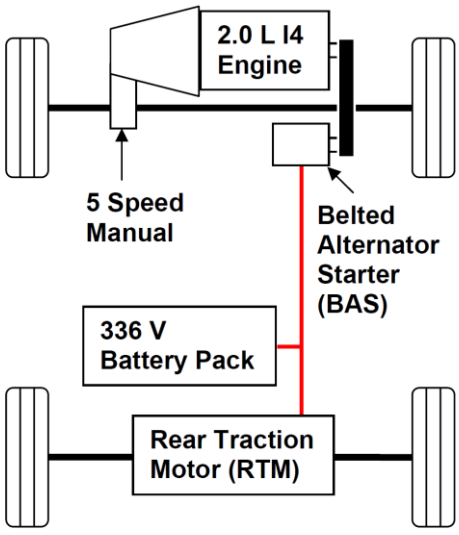

Figure 8: Split parallel architecture hybrid with belted alternator starter and rear traction motor for electric all-wheel drive

Through research of existing technology and the results from the PSAT simulation it was determined that the best package for availability and operation would be a BAS with 15 kW peak and 8 kW continuous power with a high speed of 1200 rpm. The connecting belt ratio is 2:1 with the ICE as this is good for typical high current stop/start applications. The RTM requires 60 kW of peak power and 30 kW of continuous power. The electrical system runs on a high voltage bus of about 300 V which allows for a higher peak current and electrical assist. This also reduces current draw by high voltage components decreasing losses. A low-resistance battery or collection of batteries reduces weight and transient losses. NiMHa battery pack is selected for its high peak power and its fair compromise between efficiency, performance and weight.

Parasitic loads, like AC, power steering and DC/DC voltage converter, are all electric thus reducing the mechanical load and providing better management control. The BAS provides peak torque at engine start then siphon torque for low speeds under 1000 rpm for efficient idle charging. Also it provides torque boost for transient demand and smoothing for the power range. The RTM creates AWD with a high electric power input, but limits the battery voltage to 52 kW peak power. The SPA does not have a continuously variable transmission to control engine speed which is simpler than a planetary gear transmission, like the Prius. It also does not require torque and power to be absorbed by a generator of BAS to transmit torque through the wheels. As a whole the competition vehicle has a high speed greater than 100 mph with low rolling resistance tires with a coefficient of 0.007.

The control of the electric system is dictated by the driver torque request through the throttle and brake pedals. A "positive torque request" depends on the demand of the ICE, BAS and RTM combinations that can be contributed. A "negative torque request" cannot interrupt the "fail-safe" hydraulic braking system and is managed by a proportional control strategy balancing the electrical and mechanical systems. The various engine modes and their implementation criteria developed are shown in Table 1. A similar development was required to design the ADD system.

Table 2: Hybrid electric vehicle governing control modes and criteria

Modes	Criteria
Engine Only	• under normal driving conditions • SOC too high • diagnostics or controller calibration
Engine Generate	• under normal driving conditions • SOC recharge • electrical accessories
Engine Assist	• additional torque from BAS and/or RTM to boost performance • based on pedal position, change in pedal position, vehicle speed and power train limitations • assist will vary, but not significantly during normal driving • assist will be high at higher torques and speeds to increase efficiency at "fuel enrichment" regions in typical ICE engine maps
Electric Only	• under low speeds using RTM power only • engine should not be shut down before coolant and exhaust reach operational temperatures • when engine is at operational temperatures and shut off it should not be allowed to cool down • if driver torque request exceeds RTM capacity then ICE is activated
Regenerative Braking	• activated when brake pedal is depressed • provides negative torque to send current from BAS and RTM to battery pack within power and SOC limits • recaptured energy to increase overall fuel economy rather than dissipated

Three major assumptions are made with this control strategy and design, first there are no conditions or modes for cold starting and that the vehicle functions within the power and speed limitations. The initial condition of the vehicle is assumed to be in a normal operative state and has all the components working correctly within limitations. Second, this approach does not include transmission, driveline and tire losses because it is assumed that they will be equal between the front and rear axles. Third, the SOC remains from 20% to 80% and for the start or finish the charge is provided by the conversion of fuel.

The results of this design have been categorized into two basic efficiency calculations, Conversion Efficiency (CE) and Assist Efficiency (AE). CE represents a comparison between the engine only and engine generate modes. The engine generate mode refers to the power loss to the BAS for electric power conversion. CE is the overall measure of fuel to torque efficiency which through the various simulations has an average of 34.2%. AE represents the fuel used to convert energy to the battery pack back to the BAS for electrical assist. The BAS had an average AE of 87.1 % and the RTM of 190%. If RTM AE is at 100% that means its fuel to torque efficiency was equivalent to the ICE and greater than 100% than its conversion efficiency was higher than the ICE. For regenerative braking it is difficult to calculate and determine how much energy actually makes it to charging the battery pack. The final overall CE with regenerative braking is 39%, the collection of overall results is in Table 3. Figure 9 shows the operational mode areas based on engine torque and speed for this completion vehicle.

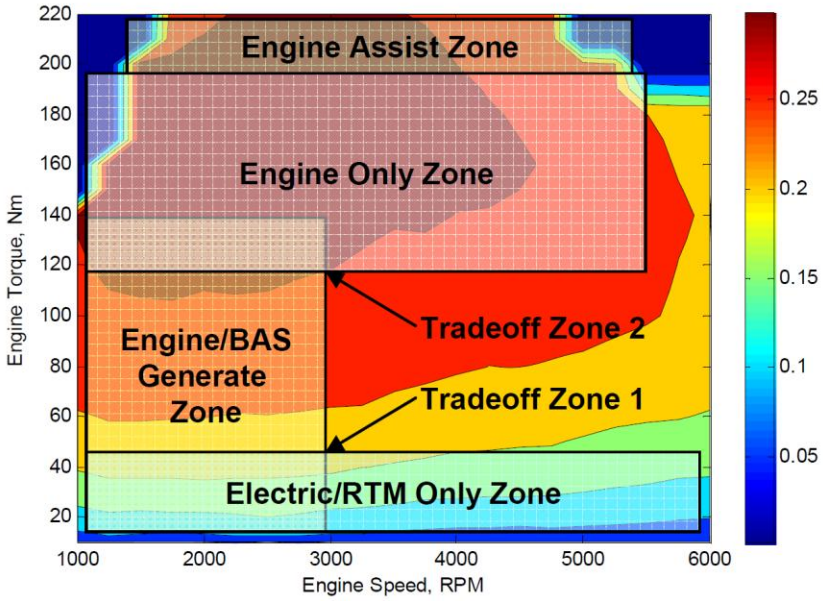

Figure 9: Operational mode areas based on engine torque and speed with an efficiency contour plot underneath shows the design is based on efficiency [19]

Table 3: Tabulated calculations for overall energy contribution of hybrid system with regenerative braking

Total stored energy	**3407 kJ**
BAS generate fuel energy needed @ 34%	10021 kJ
Regenerative braking energy contribution	407 kJ
BAS generate fuel energy needed w/regen	8824 kJ
Apparent conversion efficiency w/regen	39 %

Student competitions like Challenge X create a platform for development and progress in vehicle technology that can have a hand influencing future vehicles to have better fuel

economy and ultimately maintain vehicle appeal while reducing harmful emissions. The influence of a hybrid system on the torque efficiency of a vehicle can be seen in this study. Energy generation and conversion efficiency play a significant role in overall fuel consumption and emission of the combined power systems. This hybrid system can provide an estimated 39% energy conversion improvement by maintaining the Chevrolet Equinox ICE at higher efficiencies which is an important result.

For the ADD, the goal is to reproduce the advantages of hybrid and plug-in with the added limitation of having to work through the hitch. As such the static and dynamic loading that can be transferred to the vehicle is already set by the vehicle manufacturer. This provides an additional constraint to the overall efficiency of the ADD.

2.4 Other retrofit vehicle electrification conversions

Also in the Challenge X competition, Joseph Morbitzer [20] used a configuration that used a power split architecture to sustain electric charge. A downsized diesel engine was used with an integrated starter/alternator to drive the front wheels through an automatic transaxle and the rear wheels driven by an electric machine with a single speed gearbox, both electric motors are connected to a high voltage battery pack. The vehicle architecture was imputed into a simulator with a control strategy emphasizing priority on driver power request, to minimize fuel consumption and maintain the SOC. This approach produced significant gains, but was not as efficient when compared to a pure

electric power source. The downsized diesel motor certainly improved fuel consumption but is more suited for directly maintaining SOC.

Nathan Picot [21] in his paper took a similar approach to the Challenge X competition with a downsized diesel motor and two electric motors, but also included an exhaust after treatment and substituted a series of ultra-capacitors for the high voltage battery pack. Several control strategies were simulated covering criteria emphasizing driving cycles, conditions and habits. It was found that this approach improved drive quality as far as energy availability and management, but exceptionally performed at maintaining engine efficiency and thus ideal fuel economy of the overall system.

3 Preliminary equipment and one dimensional analysis

The approach of proof of concept testing for the ADD system, an existing SAE competition Baja vehicle is used as a first test prototype. A sensing hitch adapter to feed vehicle and towing forces is developed that is self-contained within a frame unit. A hitch adapter on the front and a ball hitch on the back for a trailer hook up allow testing the ADD concept in its entirety. A 4' by 6' road trailer completes the test assembly. Contained within the frame of the unit is a mount for an axle and housing for a rim and tire, and a belt gear to connect an electric motor. A gear ratio is required as the electric motor rpm power range is different from the road speed. The gearing is an estimate of this characteristic and chosen to be appropriate for lower speeds, which is the applicable case with the Baja vehicle. An onboard battery supplies power to the electric motor. A controller provides forward and reverse traction to optimize fuel economy. The controller is implemented using a National Instruments CompacRIO which is in turn is controlled by a computer through the use of National Instruments LabVIEW® software. A program is developed to autonomously strategize inputs from sensors and outputs to manage power and direction to the electric motor. To develop this program to correctly interpret sensor data and appropriately govern signals to the controller, a laboratory test bench is further required and described in Section 4(see Figure 22).

The Society of Automotive Engineers (SAE) competitions are held between 150 to 200 universities across North America and the world annually with several categories. The

SAE Baja acting as a test vehicle for this study can be seen in Figure 10. The vehicle suspension is relatively soft and is powered by an unmodified 300 cc Briggs & Stratton Intek 20 single-cylinder motor with a rated 10 bhp. This SAE Baja vehicle serves as the basis of the towing vehicle for the first ADD prototype testing.

Figure 10: SAE Baja competition vehicle with push plate showing used in the prototype to generate validation data for the numerical models for verification and prove concept

The power curve for the Briggs & Stratton Intek 10 hp engine used in this project can be seen in Figure 10. This range is determined by a number of physical factors, like the size of the combustion chamber and stroke length of the pistons to name a few. The ICE must interface with some type of gearing to utilize this “power band” or range of optimal efficiency. Furthermore, these gears and ratios of gearing must be appropriate to

compensate for the difference of wheel to engine speed [22]. As well there must be some form of a clutching mechanism to separate the engine from wheel rotation, as their speeds are almost always different, for instance at engine start-up or idle.

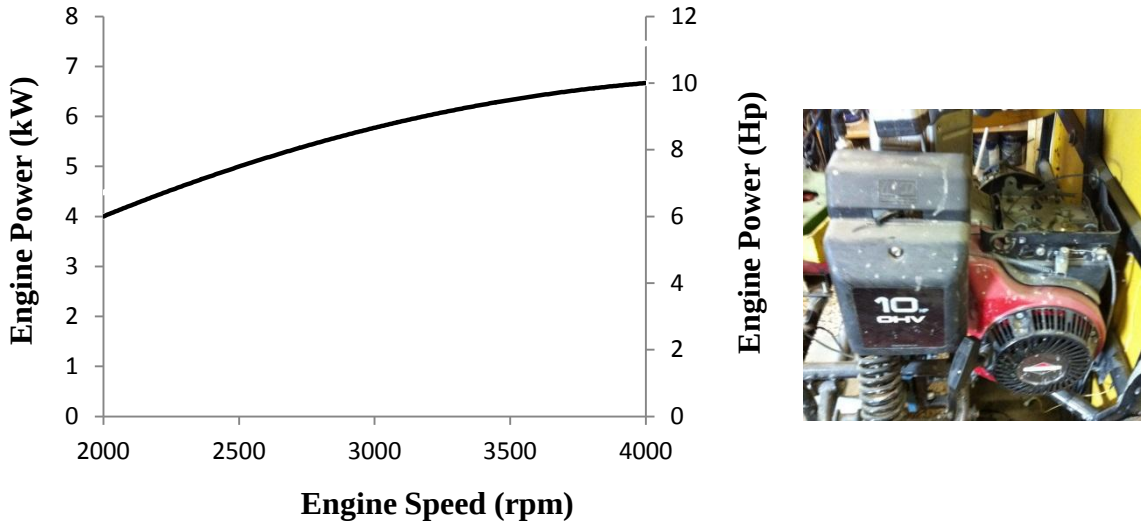

Figure 11: Briggs & Stratton Intek 10 HP performance chart on the left and image of the engine used in the prototype ADD system on the right

In typical vehicle usage, where the conventional power is an ICE, there are many stop and go. It's during these conditions of acceleration and wide variation of engine RPM that vehicle efficiency suffers. Additionally, when an engine is under heavy load like acceleration, that the most fuel is used for maximum power and burned least efficiently causing the majority of harmful emissions from a vehicle.

Electric Motors (EM) come in many variations and are classified by their internal construction, type of power used and motion generated, but simply are devices which convert electrical energy into mechanical energy. In general, EM's use magnetic field interfering attraction and repulsion forces to rotate a shaft. Internally a motor has a set of magnets facing inward, a stator, in a cylindrical configuration surrounding a round shaft, a rotor, with magnets facing outward. These magnets can be permanent magnets or electromagnets, but at least one set must be excited or controlled by electricity, AC or DC, for synchronization and continuous motion. The power delivery curve of EM's has a constant slope which maintains a fairly narrow range of efficiency when compared to ICE's.

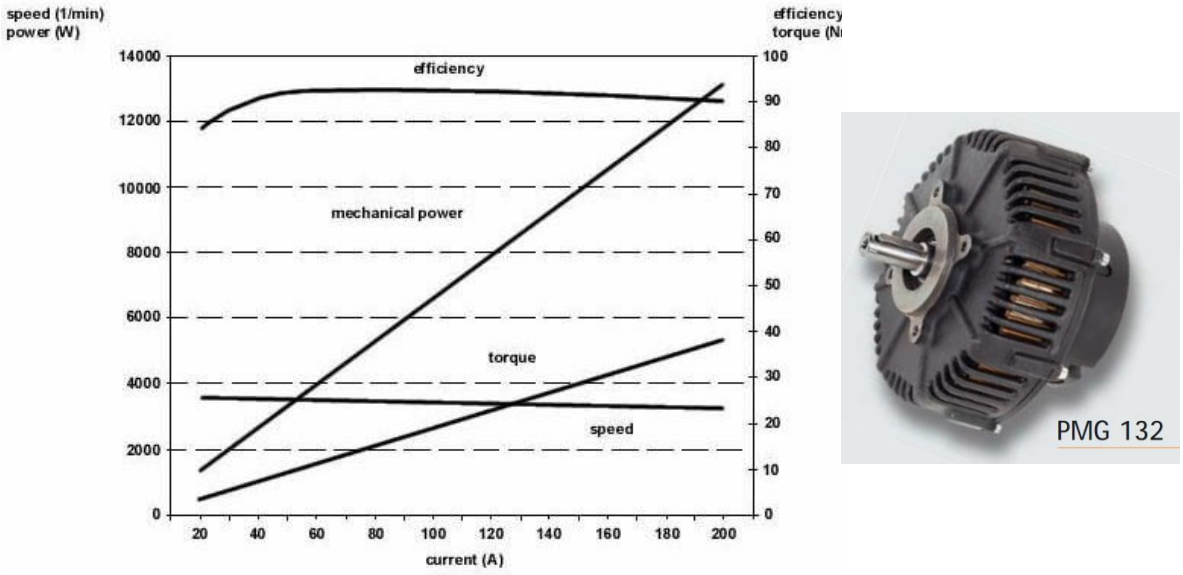

Figure 12: Permanente magnet electric motor performance chart on the left and pmg-132 picture on the right that is used to prove the ADD concept [23]

For permanent magnet motors, the stator is made from a material, like neodymium, which generates an inherent magnetic field. The rotor field is generated by excited copper wire windings around a shaft creating electro-magnets and an output torque when excited. A permanent magnet motor works particularly well for the application in the ADD because it only needs a single input voltage to function. The chart for the PMG-132 motor used is in Figure 12.

A motor controller is then connected to a power source such as a battery pack or power supply, and control circuitry in the form of analog or digital input signals shown in Figure 13.

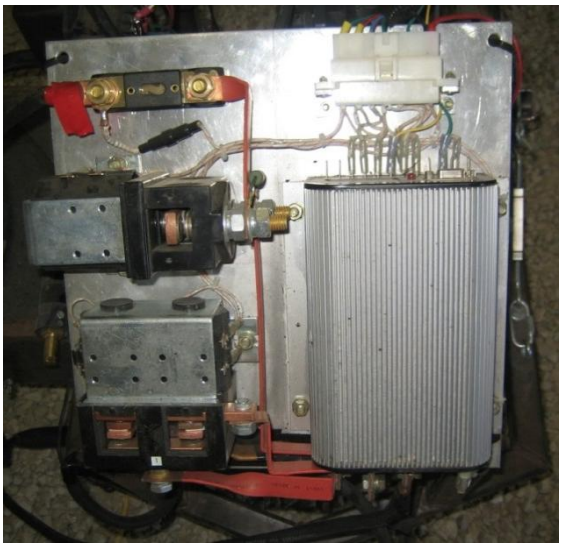

Figure 13: Controller and relays on a 38 cm^2 plate for the prototype ADD system used to test concept and provide validation data

In order to understand the function of the ADD concept between a towing SAE Baja vehicle and a trailer, a two dimensional analysis of Newton's Second Law on the individual rigid bodies is developed. The Baja, ADD and trailer are measured and calculated for their physical properties. Subsequently the overall system is mapped and run through a driving cycle to estimate the energy flow through and required by the system which is important for design, component sizing and selection, and for the resulting performance expectations.

3.1 Analytical model

The following builds the framework of equation models for the individual rigid bodies involved. Sections 3.1 and 3.2 will be combined in Section 3.3 determining estimated forces and energies developed by the system of rigid bodies.

3.1.1 Baja dimensional analysis

The SAE Baja vehicle differs significantly in shape, body and aerodynamics from typical production vehicles and yet the same analysis and Equation 3.1.1-1 can be applied to both.

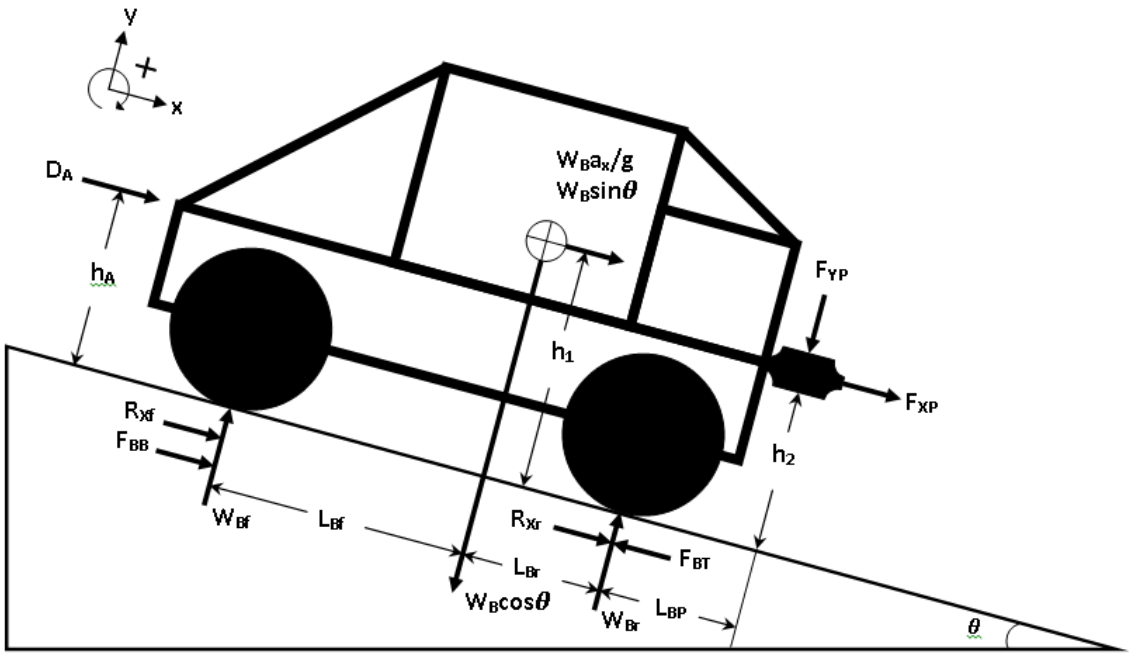

Figure 14: SAE Baja towing vehicle force balance used in static model

Moment of torque about the vehicle rear wheel contact point:

$$\sum T_B = 0 \Rightarrow (W_B \sin\theta)h_1 + \left(W_B \frac{a_x}{g}\right) h_1 - (W_B \cos\theta)\, L_{Br} + W_{Bf}\left(L_{Bf} + L_{Br}\right) + D_A h_A + F_{XA} h_2 + F_{YA} L_{BP} \quad \text{3.1.1-1}$$

The aerodynamic drag force, D_A, is defined as,

$$D_A = \frac{1}{2} C_D \rho A_F v^2 \qquad 3.1.1\text{-}2$$

Sum of the forces in the *y*-direction:

$$\sum F_y = 0 \Rightarrow W_{Bf} + W_{Br} - F_{YA} - W_B \cos\theta. \qquad 3.1.1\text{-}3$$

Sum of forces in *x*-direction:

$$\sum F_x = 0 \Rightarrow W_B \sin\theta + W_B \frac{a_x}{g} + R_{Xf} + R_{Xr} + F_{BB} - F_{BT} + F_{XA} + D_A. \qquad 3.1.1\text{-}4$$

Rolling resistance, R_X, is defined as,

$$R_X = C_{rr} W = C_{rr} M g \qquad 3.1.1\text{-}5$$

Subsequently, the rolling resistance forces on front and rear axles, R_{Xf} and R_{Xr}, respectively, are defined as:

$$R_{Xf} = C_{rr} W_{Bf} \quad 3.1.1\text{-}6$$

$$R_{Xr} = C_{rr} W_{Br} \quad 3.1.1\text{-}7$$

The brake force to the ground necessary for the vehicle to maintain a given deceleration at any moment is:

$$F_{BB} = -W_B \sin\theta - W_B \frac{a_x}{g} - R_{Xf} - R_{Xr} + F_{BT} - F_{XA} - D_A \quad 3.1.1\text{-}8$$

The torque to the ground necessary for the vehicle to accelerate at any moment is:

$$F_{BT} = W_B \sin\theta + W_B \frac{a_x}{g} + R_{Xf} + R_{Xr} + F_{BB} + F_{XA} + D_A \quad 3.1.1\text{-}9$$

3.1.2 ADD dimensional analysis

The ADD rigid body analysis differs from the Baja in that it only has a single wheel for which to provide torque, positive or negative, as in braking. It is also assumed that the aero dynamic drag will be negligible because of its small form factor and the vehicle in front will provide the entire frontal area of drag for the system.

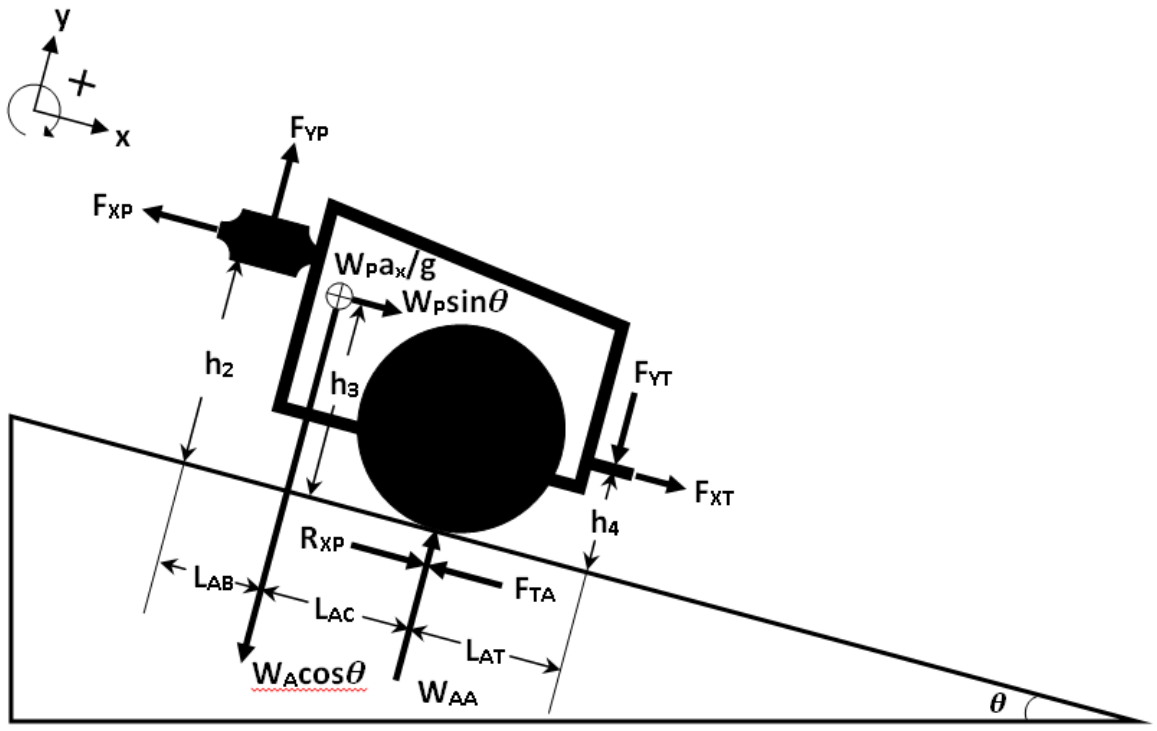

Figure 15: ADD force balance used in static model

Moment about the ADD wheel contact point:

$$\sum T_A = 0 \Rightarrow (W_A \sin\theta)h_3 + \left(W_A \frac{a_x}{g}\right) h_3 - (W_A \cos\theta)\, L_{AC} + F_{XT}h_4 + F_{YT}L_{AT} - F_{XA}h_2 + F_{YA}(L_{AB} + L_{AC}) \quad 3.1.2\text{-}1$$

Sum of forces in *x*-direction:

$$\sum F_x = 0 \Rightarrow W_A \sin\theta + W_A \frac{a_x}{g} - F_{XA} + R_{XA} - F_{TA} + F_{XT} \qquad 3.1.2\text{-}2$$

Sum of the forces in the *y*-direction:

$$\sum F_y = 0 \Rightarrow F_{YA} - F_{YT} + W_{AA} - W_A \cos\theta \qquad 3.1.2\text{-}3$$

ADD Rolling resistance, R_{XA}, is defined as:

$$R_{XA} = C_{rr} W_A = C_{rr} M g \qquad 3.1.2\text{-}4$$

3.1.3 Trailer dimensional analysis

The trailer is a passive body, only contributing a towing load that will not provide torque through the wheels, positive or negative. It is assumed again that any drag force will be on the towing vehicle frontal area because of the low speeds and the trailer will be a simple frame with wire meshing.

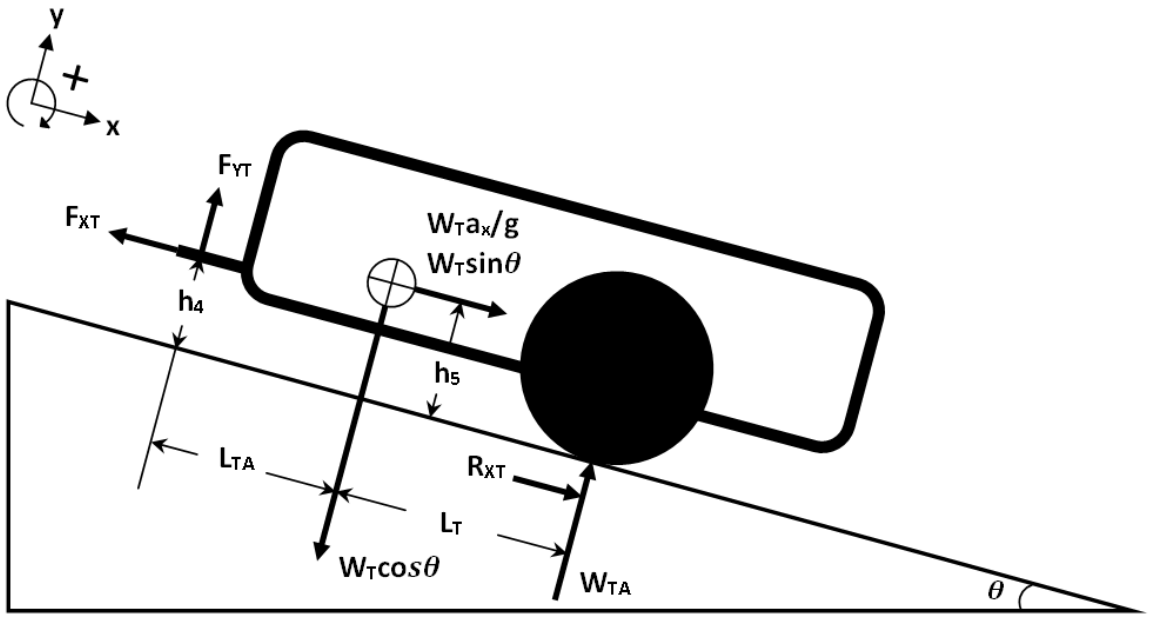

Figure 16: Towing trailer force balance used in static model

Moment about the trailer wheel contact point:

$$\sum T_T = 0 \Rightarrow (W_T \sin\theta)h_5 + \left(W_T \frac{a_x}{g}\right) h_5 - (W_T \cos\theta)\, L_T - F_{XT} h_4 + F_{YT}(L_{TA} + L_T) \qquad 3.1.3\text{-}1$$

Sum of forces in *x*-direction:

$$\sum F_x = 0 \Rightarrow W_T \sin\theta + W_T \frac{a_x}{g} + R_{XT} - F_{XT} \qquad 3.1.3\text{-}2$$

Sum of the forces in the *y*-direction:

$$\sum F_y = 0 \Rightarrow F_{YT} + W_{TA} - W_T \cos\theta \qquad 3.1.3\text{-}4$$

Trailer Rolling resistance, R_X, is defined as,

$$R_{XT} = C_{rr} W_T = C_{rr} Mg \qquad 3.1.3\text{-}5$$

3.2 Initial measurements and calculations

Initial measurements are taken using weight scales and a measuring tape, with some of the other values are given by physical inherencies, based on assumptions or basic calculations. It is assumed that the testing area will be flat and in the Winnipeg, MB area, the conditions are shown in Table 4.

Table 4: Baja with ADD system and trailer model ambient conditions

	Symbol	Value	Unit
Gravity	g	9.83	m/s^2
Standard air density	ρ	1.22	kg/m^3

3.2.1 SAE Baja

The SAE Baja vehicle measurements are as follows. Table 5 is the weight of the vehicle on the front and rear tires separately as well as the wheel base length and the rear axle to center of push plate. These measurements are required for calculating the driving forces as well as the subject forces on the push plate in Equations 3.1.1-1, 3.1.1-3, and 3.1.1-4.

Table 5: Baja physical measurements for the model analysis

		Symbol	Value	Unit
Weight	Front axle	W_{Vf}	73.48	kg
	Rear axle	W_{Vr}	136.5	kg
	Driver	W_D	113.4	kg
	Total	W	323.4	kg
Length	Wheelbase	$L_{Bf} + L_{Br}$	1.727	m
	Rear axle to push plate	L_{BP}	0.3810	m

Table 6 is the coefficients and frontal area for which the aerodynamic drag and the resistance to motion can be determined, and required in Equation 3.1.1-2. The Baja rolling resistance coefficient used to calculate rolling resistance in Equation 3.1.1-5. The Baja frontal area and coefficient of drag are used in the Equation 3.1.1-2 to determine overall drag, D_A, for Equation 3.1.1-4. The aerodynamic drag from the Baja is assumed to be the only significant negative aerodynamic force as the ADD and trailer will be much lower and relatively small. The rolling resistance R_{Xf} and R_{Xr} are calculated using the weights in Table 6, Table 5 and Equation 3.1.1-5. The Baja frontal area is measured with a measuring tape. The coefficients of drag and rolling resistance are taken from an SAE source [24] for Baja vehicles in competition for the same type and shape of vehicle.

Table 6: Baja negative force coefficients for equations in the model analysis

	Symbol	Value	Unit
Rolling resistance coeff.	C_{rr}	0.048	
Front rolling resistance	R_{Xf}	3.528	kg
Rear rolling resistance	R_{Xr}	6.554	kg
Baja frontal area	A_F	1.100	m^2
Coeff of drag	C_D	0.700	

The Baja drive train between the ICE and wheels consists of a belt clutch to a chain gear, then the rear axle going to CV joints to each wheel. The ratio and efficiencies are listed in Table 7.

Table 7: Baja drive train efficiencies for the model analysis [2]

	Symbol	Value
Chain gear ratio	G_B	5
Belt clutch efficiency	E_B	0.80
Chain gear efficiency	E_C	0.98
Drive train efficiency	E_D	0.90
Overall efficiency	E_T	0.71

The maximum braking force, F_{BB}, is estimated from other SAE Baja vehicles with similar braking components and configurations at 234.6 N-m [20].

3.2.2 ADD

The initial measurements for the ADD designed for the tests are as follows. Table 8 is the weight, height and length which are required for the calculation of applicable Newtonian forces in Equations 3.1.2-2 and 3.1.2-3.

Table 8: ADD physical measurements for the model analysis

		Symbol	Value	Unit
Weight	ADD total	W_P	99.78	kg
Height	CoG to ground	h_3	0.3556	m
	Hitch to ground	h_4	0.6604	m
Length	Hitch to CoG	L_{PB}	0.6096	m
	Hitch to axle	L_{PC}	0.6604	m
	Hitch to trailer hitch	L_{PT}	1.016	m

The significant negative force on the ADD is assumed to be only R_{XP} as it will be headed by the much larger Baja and will likely be in the low pressure zone following the vehicle. The required coefficient, C_{rr}, is in Table 9. R_{XP} is calculated in Equation 3.1.2-4 and is required in Equation 3.1.2-2.

Table 9: ADD negative forces for equations in the model analysis

ADD Forces	Symbol	Value	Unit
Rolling resistance coeff.	C_{rr}	0.015	
Rolling Resistance	R_{XP}	4.790	kg

Through belt gear between the EM and the axle there is a gear ratio and losses in efficiencies shown in Table 10.

Table 10: ADD belt gear ratio and efficiency for the model analysis

Parameter	Symbol	Value
Belt gear ratio	G_P	8
Belt gear efficiency	E_{PB}	0.95

The EM, controller and batteries ratings are in Table 11. These are the specified ratings provided by the manufacturer and the combination of them in the configuration used. The maximum discharge rate is an industry standard rating noted by the term, C.

Table 11: ADD electric power source ratings for the model analysis

Measurement		Symbol	Value	Unit
Battery Source	Nominal voltage	V_P	12.0	V
	Number of batteries	N_B	4	
	Discharge rating	I_B	4.00	Ah
	Max discharge rate	C_B	1.00	C
Source Control	Proportional coeff	P_P	0.80	

3.2.3 Trailer

The weight, height and length measurements for the trailer are in Table 12 and are used in Equations 3.1.3-2 and 3.1.3-3.

Table 12: Trailer measurements for the model analysis

Trailer Measurements		Symbol	Value	Unit
Weight	Trailer	W_T	206.4	kg
	Additional	W_{TA}	31.75	kg
	Total	W_{TT}	238.1	kg
Height	Trailer CoG	h_5	0.4064	m
	Trailer hitch	h_4	0.3556	m
Length	Trailer hitch to CoG	L_{TP}	1.219	m
	Trailer hitch to axle	L_T	1.270	m

Similarly, the significant negative force on the trailer is only R_{XT} and the required coefficient, C_{rr}, is in Table 13. R_{XT} is calculated in Equation 3.1.3-4 and is required in Equation 3.1.3-2.

Table 13: Trailer negative forces for the model analysis

Measurement	Symbol	Value	Unit
Rolling resistance coeff.	C_{rr}	0.015	
Rolling resistance	R_{XT}	6.191	kg

3.3 System model analysis

A spreadsheet model is constructed from the reduced equations in Section 3.1 and the measurements in Section 3.2. With a given velocity curve, the equations are arranged to determine positive or forward forces required by the two motors to overcome the weight of the trailer and negative forces of rolling resistance, drag and vehicle weight.

3.3.1 Power source analysis

The ICU on the Baja and the EM on the ADD have to be mapped as far as their torque contributions to the overall system when towing a load. Figure 17 and Figure 19 have the power and torque curves of the ICU and EM, respectively. The bend in the curve of the ICU is noticeable as for power it begins to plateau about two thirds into the engine speed range and one third for engine torque. In contrast for the EM, the power and torque curve are linear throughout the motor speed range. This is an inherent characteristic of ICU's versus EM's. Section 1.4 explains how ICU's have a power range for engine speed because of the engine geometry and the conversion of combustion to mechanical forces.

Whereas, Section 1.4 reveals how EM's inherently convert electromagnetic forces directly to rotational motion (ie. power and torque).

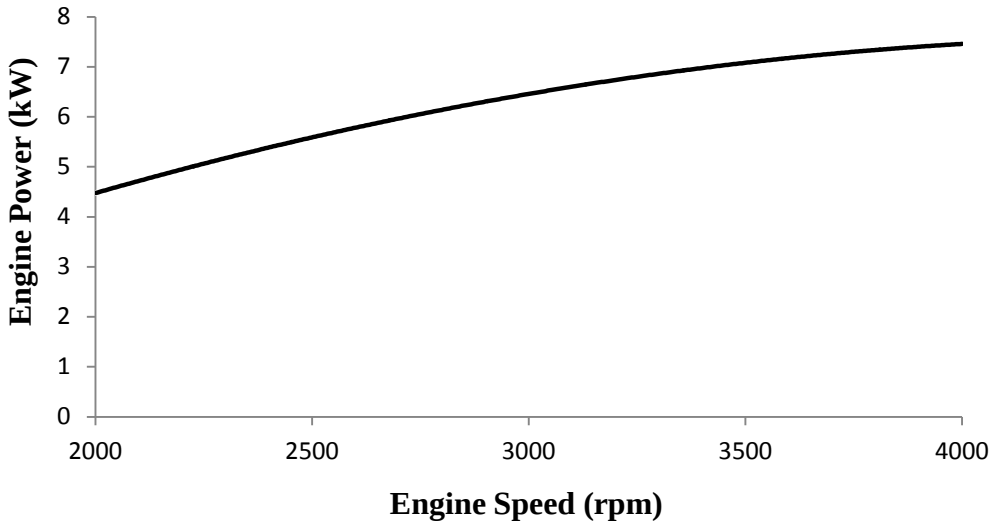

Figure 17: Briggs and Stratton 10.0 HP motor power performance chart [25] installed in the SAE Baja towing vehicle for the ADD prototype

The equation for the power curve in Figure 17 was determined using a 2nd order polynomial fit. The equation for the horsepower is

$$Engine\ Power\ (Hp) = -5x10^{-7} * (Engine\ Speed)^2 + 0.0044 * (Engine\ Speed) - 2.442 \qquad 3.3.1\text{-}10$$

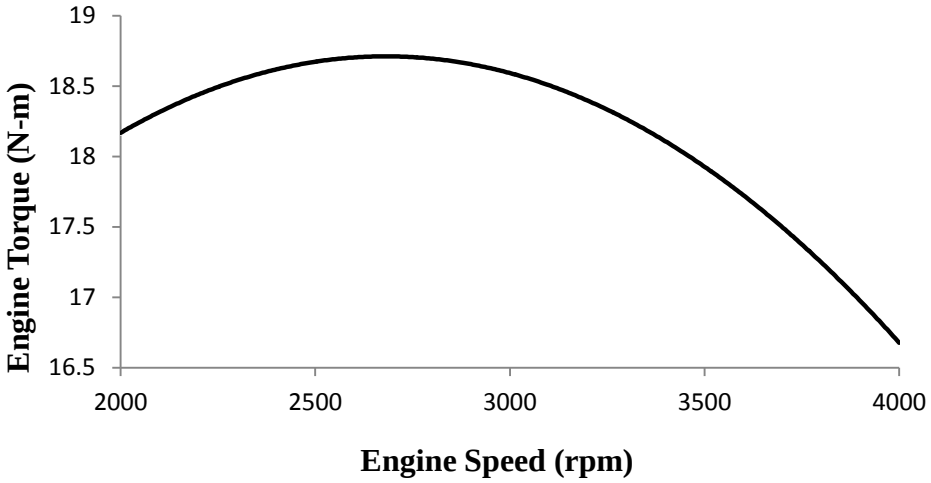

Figure 18: Briggs and Stratton 10.0 HP motor torque performance chart [25] installed in the SAE Baja towing vehicle for the ADD prototype system

The equation for the torque curve in Figure 17 was determined using a 2nd order polynomial fit. The equation for the torque is

$$Engine\ Torque\ (lb-ft) = -1x10^{-6} * (Engine\ Speed)^2 + 0.0063(Engine\ Speed) + 10.303 \quad \text{3.3.1-11}$$

Similarly from Figure 12 in Section 1.4, for the EM on the ADD, an equation for the torque curve is determined using a 1st order linear approximation as it resembles a straight line, which is common for EM's.

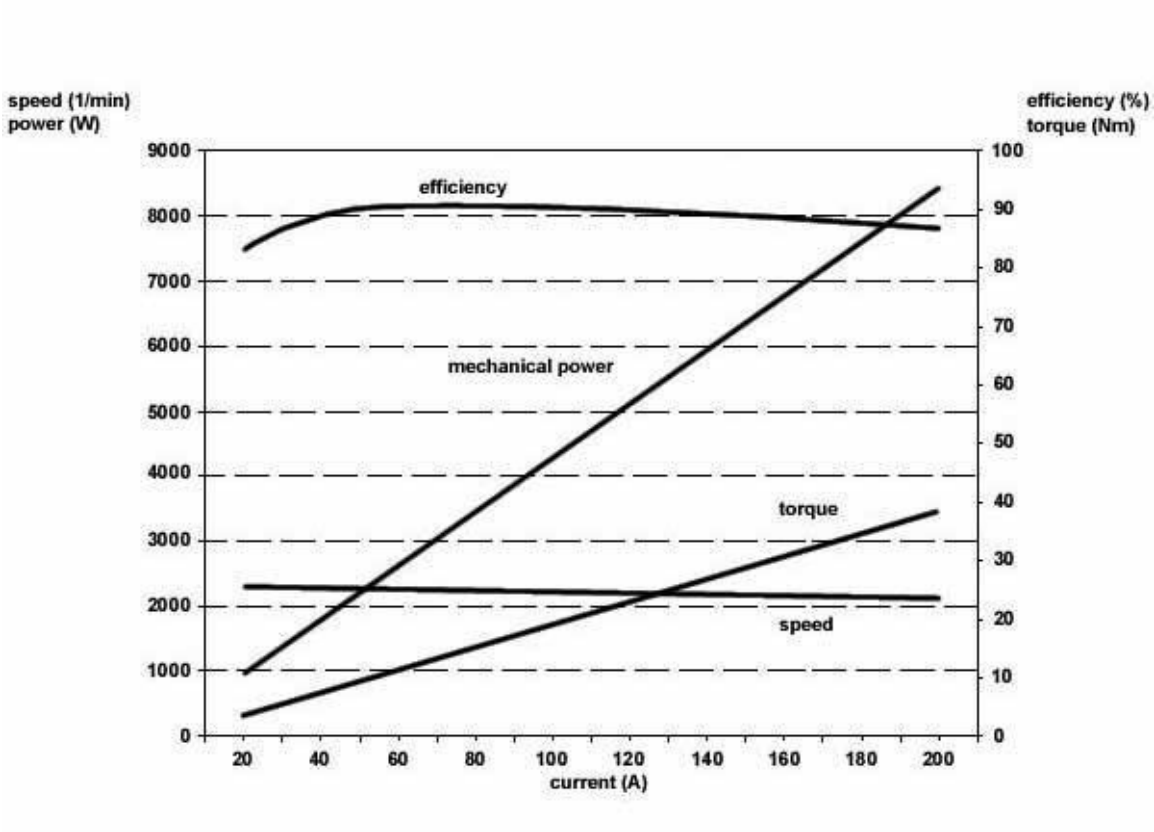

Figure 19: Power curve of PMG 132 electromagnetic motor [23] used in the ADD prototype

The equation determined from Figure 19 is as follows

$$EM\ Torque\ (lb-ft) = 0.1434 * (current) + 0.082 \qquad 3.3.1\text{-}12$$

Under these conditions, the maximum torque of the EM is limited by the combined discharge of the batteries, which is 16 A. Using Equation 3.1.2-2 the maximum torque of

the EM is 3.227 N-m and at the wheel will be 25.77 N-m because of the 1:8 ratio of the belt gears.

3.3.2 Model control inputs

In reality, an actual vehicle will have two inputs that dictate the torque contribution, whether positive or negative, to the system, otherwise known as throttle and brake pedals. In the analytical point mass model these inputs are derived from a quarter of a sine wave multiplied by the engine speed for throttle or braking force for a brake. It is reasonable to assume that typically a human foot on a pedal will follow this curve as to avoid the discomfort of abrupt motion of the vehicle. The throttle and brake curves can be seen in Figure 20.

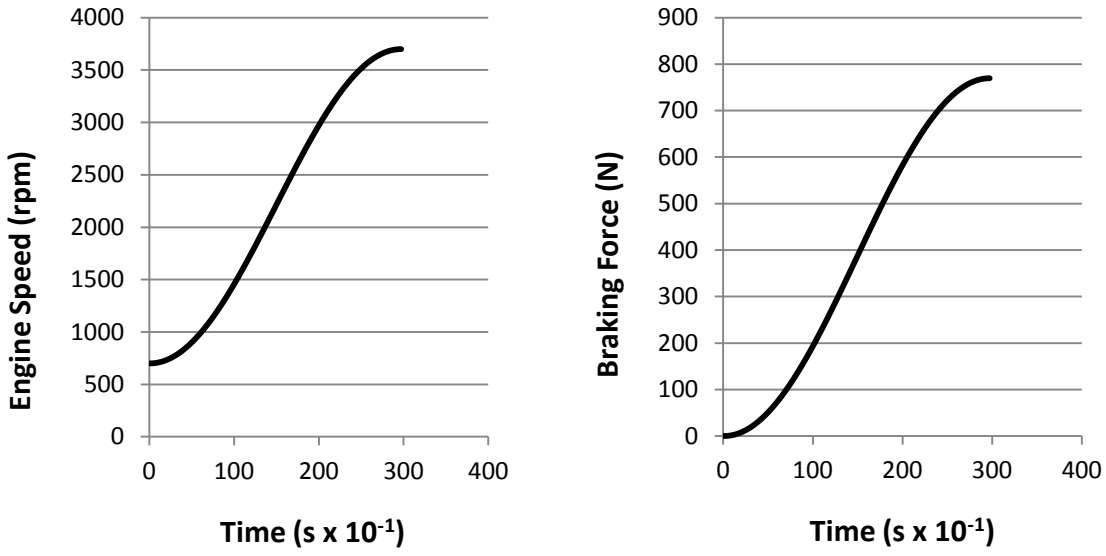

Figure 20: Throttle input curve on the left and braking input curve on the right

The throttle curve is used until a top speed is reached then the brake curve implements until it stops the vehicle or vehicle train. This should yield a single cycle of the vehicle simulation values that should be important as a comparison of actual test results.

3.3.3 Model results

Compiling together the Equations in Section 3.1 and 3.3.1 and inputting the parameters in Section 3.2 and 3.3.2 we get the velocity curves in Figure 21.

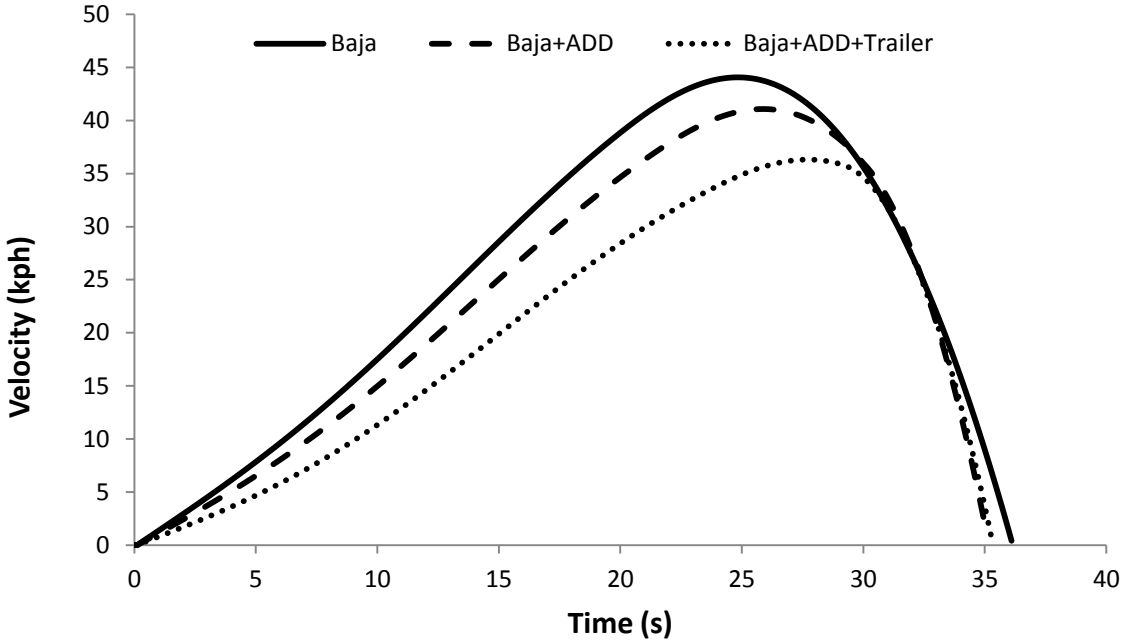

Figure 21: Velocity from each run from the static force balance model

The velocity curves from the spreadsheet analysis show that the Baja alone has the top speed followed by the Baja and ADD, then the Baja with the ADD and Trailer attached. When the energy exerted or torque provided by the ICE in the Baja vehicle is summed and divided by the weight of the system, we get the results shown in Table 14.

Table 14: Torque exerted by Baja vehicle

	Baja1	Baja+ADD	Baja+ADD+Trailer
Torque by weight	6.833 N-m	4.976 N-m	2.901 N-m
Difference		27.2%	57.5%
Comparative difference			30.2%

Table 14 shows that overall, on a weight basis, through the run 6.833 N-m of torque is contributed to the velocity for the Baja vehicle alone, whereas for the Baja and ADD only 4.976 N-m of torque is contributed and 2.901 N-m for the Baja with the ADD and Trailer attached. This is a difference of 27.2% for the ADD attached and 57.5% for the ADD and trailer attached. In other words, with the addition of the ADD it reduces the overall energy required by 27.2% to propel the vehicle for the same period. Likewise, for the addition of the ADD and trailer there is a 57.5% reduction in energy required leaving a significant difference of 30.2% between them. This is possible because with addition of the trailer weight the ADD contributes more torque to compensate for the load of the trailer.

4 Laboratory and experimental testing

4.1 Laboratory test bench apparatus

4.1.1 Physical apparatus

The purpose of the laboratory test bench apparatus is to validate the push plate as well as to learn and develop a lead-follow PID strategy using LabVIEW®. The setup can be seen in Figure 22. The main structure of the apparatus is a tubular steel frame that is designed and welded in order to accommodate two Linak LA36 linear actuators and be bolted to a large table. The system is controlled by LabVIEW® where sensor data is read and reacted to through the same CompactRIO from the field apparatus.

Figure 22: Laboratory test bench used to test the control system for the push plate with the left actuator representing the towing vehicle and the right actuator representing the ADD

The actuators are controlled individually by 10 VDC controllers, which had to be manually calibrated by integrated potentiometers to limit linear motion and force. The system is powered by two 12 VDC motorcycle batteries, the same that are used on the field apparatus. Then the voltage is conditioned by circuits that are built for the 10 VDC required by the push plate and other sensors. In the cases where the voltage needs to be stepped down, voltage bridges are used. In other instances, a constant supply is required and voltage regulators are integrated, and shown in Figure 23.

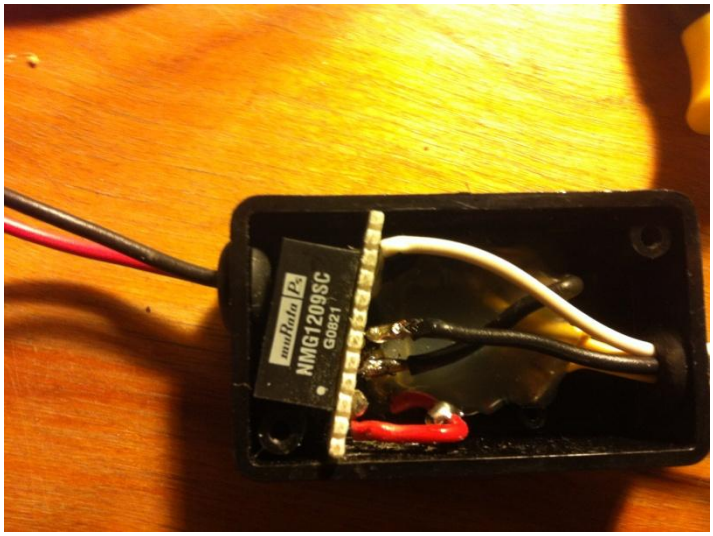

Figure 23: Voltage regulator circuit installed for the sensors on the test bench and position control on the linear actuators

The actuators require a constant 24 VDC power supply which is connected to a 120 VAC wall outlet. For safety, there were emergency stop position sensors on the upright posts in the middle of Figure 22 to protect against over run and irreparable damage. The rated force of the actuator is 10,000 N which could tear apart the steel frame and table. Each actuator also provides inherent position feedback which can be read by LabVIEW®. The main black box in the middle of Figure 22 contains the manual power on/off switch, LED indicators and fuses for circuit protection.

Below each actuator are DC/DC controllers that are also powered by 12 VDC batteries from the field apparatus. LabVIEW® will send an analog 0 to 5 VDC signal for speed of movement and digital signals for braking and forward or reverse motion. The controllers

will then convert the signals to open or instantaneous opposition motion for brake, up to 24 VDC for forward motion and as low as -24 VDC for reverse motion.

4.1.2 Data acquisition and software apparatus

The CompacRIO and LabVIEW® software on a PC Desktop are setup as follows. The cRIO has two levels of processing and control. The first level is base level program stored on the cRIO that runs the FPGA system. It is able to work autonomously without communication lag or unnecessary logging. It has limitations and can only process to the maximum number of clock signals remaining after the necessary internal functions. It can however react fast to inputs and process controls at 1 kHz when provided, however, for larger more complicated tasks, such as PID controls, its operation is restricted. Data cannot be monitored or logged effectively at this frequency, by a chart or otherwise, only the basic real-time values are displayed and log space is limited.

The LabVIEW® software similarly has two levels, there is a graphical programming interface which is the framework for building user software and there is a customizable graphical user interface where monitoring and pseudo- manual control can be arranged. Both of the LabVIEW® levels for the cRIO are displayed in Figure 24.

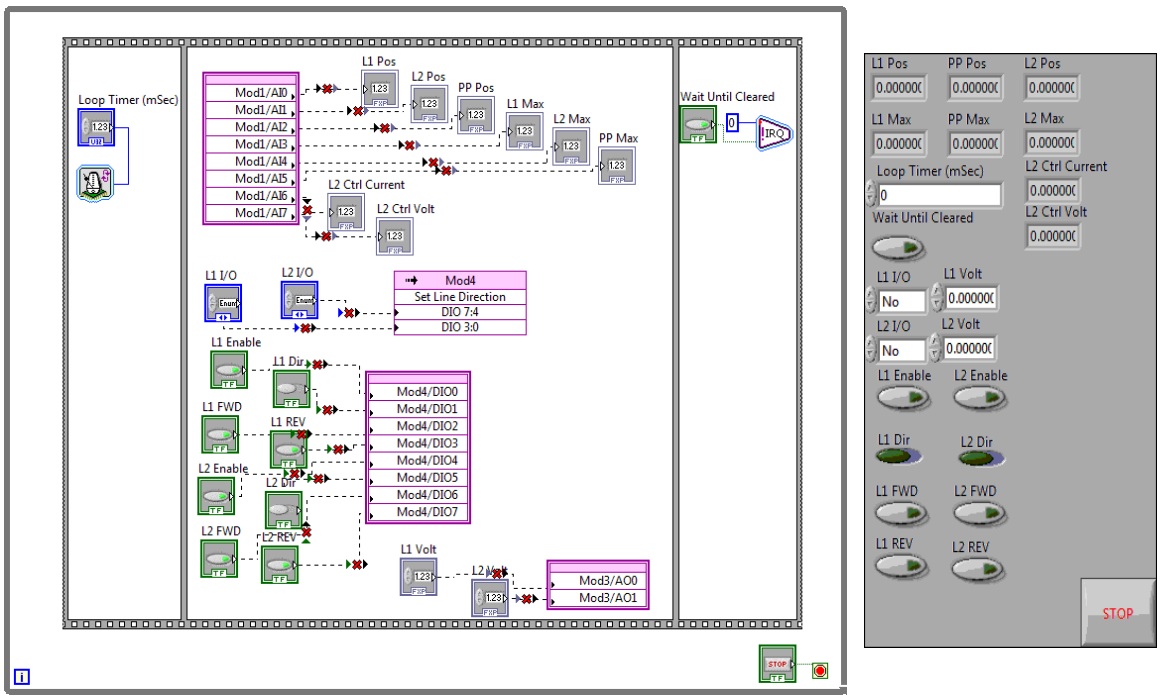

Figure 24: cRIO graphical programming interface used in the test bench to implement the push plate feedback control loop strategy later installed on the ADD prototype

The test bench required software to be operating on the FPGA and PC platform. The program on the cRIO is setup to read the sensors and feed them to the program on the PC with the higher level PID controls are able to be calculated then sent back to the cRIO. At the PC level, it is also possible to log large amounts of data and monitor charts of sensor data, inputs and controls slightly behind real-time. It is limited by the cRIO's ability to process and send data, data transmission is inherently a lower priority to functional tasks, hence is clock cycles are scarce then it is delayed until it is able to send communication. In some cases, this might be unattainable and the cRIO becomes

inaccessible as it tries to manage more tasks than resources to process them. An image of the PC graphical program and interface are shown in Appendix A.

4.2 Laboratory test procedure

A program is developed in LabVIEW® to read the position signal from the actuators and the push plate while providing a signal to the controllers. First, the push plate would be fixed to the linear actuators with lynch pins and power to the test bench turned on. Then the actuators have to be calibrated to sit in the middle of the frame between the actuators as to not allow the motion to overrun the physical limits of the frame and cause damage to it or the push plate. The calibration is done by manually setting the motion in LabVIEW® for the actuators to move the push plate to the acceptable limits of motion and then set the voltage value of the position as a software stop. The software is designed to read the physical lever switches to know if they are triggered. The lever switches are wired to cut power to the controllers and actuators in event of triggering.

The program is set to run automatically, by having the lead actuator move and then the other actuator follow the motion based on the PP offset. The voltage potential from the push plate linear potentiometer is then read to determine the offset displacement. A PID controller in LabVIEW® is tuned to govern the motion of the process. First the PID reads the offset of the push plate caused by the sine wave motion of the lead actuator, and then processes the feedback to subsequently send a forcing signal to the follow actuator to

neutralize the displacement. The lead actuator signal follows a sine wave forcing roughly 30 mm of reciprocating motion. Then the signal is monitored and logged in the LabVIEW® software.

4.3 Laboratory test results

The data for the Lab test with opposing linear actuators is shown in Figure 25. The lag and over/under shoot is created by the discrepancy in the forward and reverse velocity of the each actuator. The linear actuators move faster in forward than in reverse, as can be seen by the narrow lag on the upswing and the wider lag on the down swing. This graph primarily validates the PID strategy and code developed to establish appropriate ADD inputs on neutralizing the differential created by the trailer sensed by the push plate.

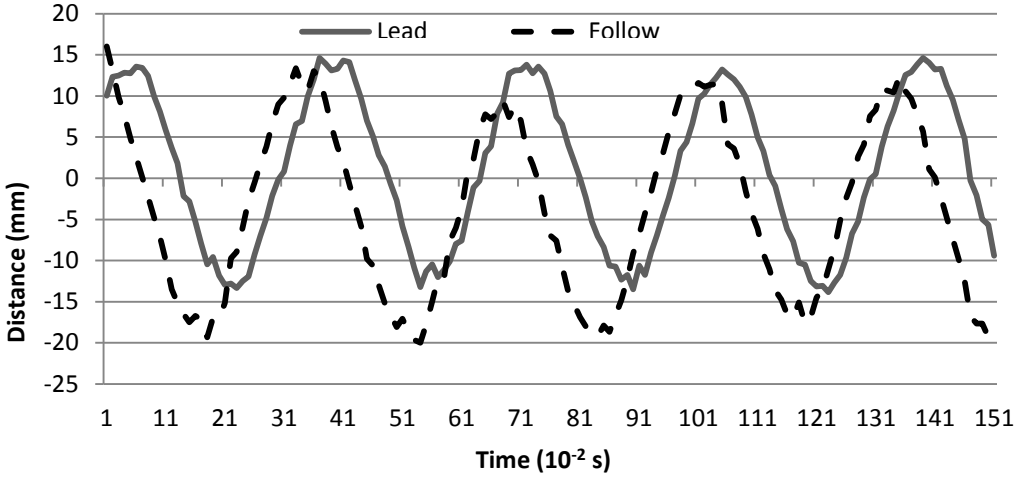

Figure 25: Lead-follow PID strategy laboratory data obtained from the test bench

5 Experimental field testing

5.1 Field prototype experimental apparatus

The field apparatus consists of three basic components and electronics. First, the main driving component, the Baja vehicle with all of its wired sensors, cRIO and a laptop to log and control the process. Second, the ADD with its wired sensors, controller, battery pack and EM, all connecting to the cRIO on the Baja vehicle. Third, is the trailer, a passive component, a simple metal frame trailer with weights. The setup can be seen in Figure 26.

Figure 26: The Baja, ADD system with push plate, and trailer prototype

5.1.1 Baja

The power for the Baja vehicle is generated by a Briggs & Stratton Intek 10 hp side shaft motor, as seen in Figure 27. The engine is attached in the right rear of the Baja above the right rear suspension. The working shaft protrudes out of the rear of the engine and is not clearly seen in the figure.

Figure 27: Briggs and Stratton Intek 10 hp motor installed and monitored in the prototype towing vehicle experimental apparatus

From the working keyed shaft of the engine, the clutch is fitted and connected with a belt to friction spindle that increases the radius of the belt as the rotational speed increases. The clutch also moderately increases the radius of belt travel. However, after

engagement and at operating speeds the ratio between the clutch and spindle remains constant. The belt of the clutch has tapered edges which allow for the friction on the clutch and spindle which can be seen in Figure 28.

Figure 28: Rear angle of Baja ICE to axle setup configuration used in the first scaled prototype of the ADD system

The rate at which the clutch engages is determined by three small weighted cams and the engaging RPM is governed by a loaded spring. The clutch is from a Polaris® snow machine with about a 120 HP engine. The Briggs & Stratton has only 10 HP, so the clutch had to be rebuilt with a new weight spring so that it would engage at a more appropriate lower rotational speed of about 800 rpm. Figure 28 shows the clutch on the side shaft of the ICE then a belt from the clutch to a spindle gear on a shaft with a chain gear.

Figure 29: Engine RPM sensor on the left and ADD axle RPM sensor on the right located on the towing vehicle

On the left of Figure 29 shows the engine rpm optical speed sensor with the reflective tape seen close to the working shaft on the face of the clutch for a direct reading. On the right is an identical optical speed sensor on the ADD axle also with the accompanying reflective tape. The axle RPM sensor views the axle directly and has a custom nozzle because of the angle and to shade excessive ambient light, such as bright sunlight, which interferes with readings. Both sensors use infrared to read optical pulse reflections off of the special patches on the rotating shaft faces.

5.1.2 ADD

The original ADD design was spatially conceptualized in SolidWorks® to determine if and how the expected components would fit together and in a form that was suitable for testing this concept appropriately. The PMG-132 EM is chosen for its form factor,

reliability as a brushless motor and ease of control with permanent magnets. The synchronous drive gearing is based on the relative speed of the EM versus the road speed. The gel cell batteries are inexpensive, reliable and easily available. The first concept is shown in Figure 30 and was originally referred to as the Plug-in Electric Trailer (PET) instead of the ADD system.

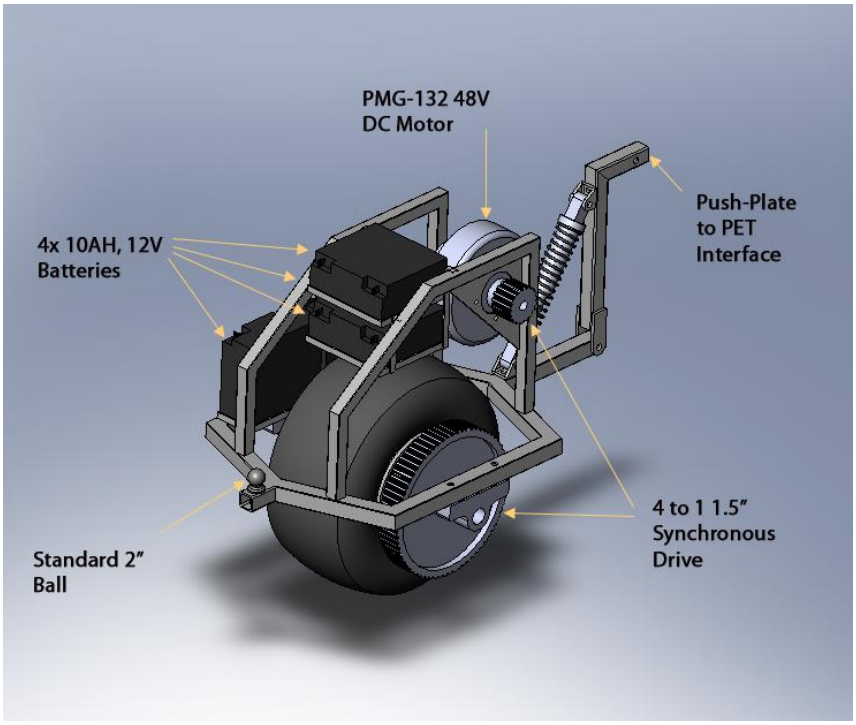

Figure 30: The first Auxiliary Drive Device concept diagram configuration as implemented in the experimental scaled prototype

The frame is welded together from 1¾ inch square steel tubing. The angled suspension is at 45 degrees and is a shock and damper used for a motor bike. In Figure 31, the left picture has the concept model designed in SolidWorks® and on the right is the actual

ADD built. On the left side of the frame is the battery pack containing four 12 VDC gel-cell batteries as used in smaller vehicle like motorcycles and ATVs. The battery pack also has 600 A welding cable with welding coupling to allow for convenient exchange of the batteries. The “pancake” cylindrical PERM electric motor provides thrust through a notch belt with an 8:1 gear ratio increase. On the back of the frame is the DC/DC controller with forward and reverse relays and a current shunt for protection. The small rectangular box on the upper left part of the frame on the actual ADD is a DC converter to interface the voltage signals from the sensors and controller to the CompacRIO.

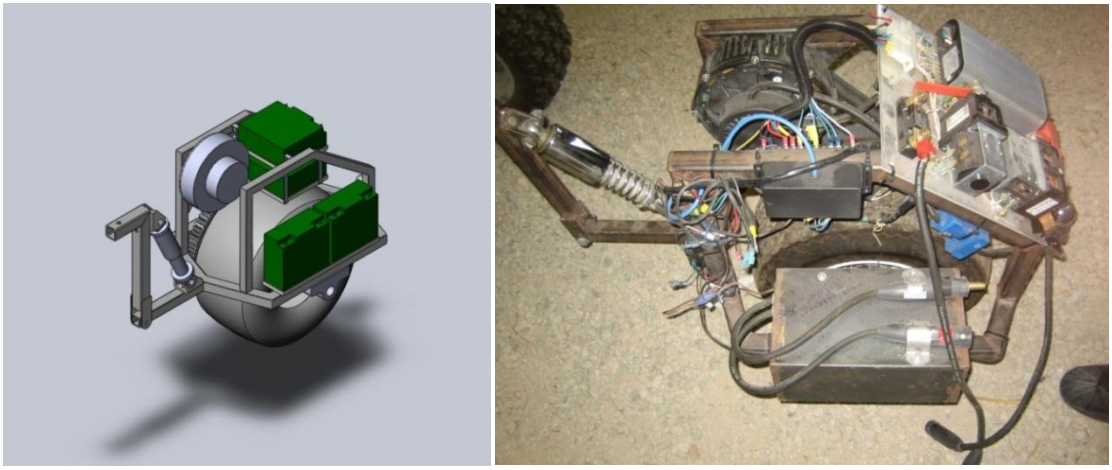

Figure 31: ADD 3-D CAD model on the left, and final design implementation on the right with data acquisition system and connected to the push plate and towing vehicle (see Figure 33)

5.1.3 Push plate

The concept of the push plate is a device that measures the force of a trailer load on a towing vehicle. The method is to measure the voltage through a linear potentiometer, which is fragile, inside of housing strong enough to sustain extended vehicle loading. Two overlapping plates connected on opposite sides with linear bearing between them. Over the linear bearings are springs to sustain large motion and forces, but still allow the linear potentiometer the full range of measurement. The plate on the Baja side is larger as it is connected to a pivot allowing some rotational motion for turning and rough roads. Rubber bumpers across the pivot between the larger plate and the rigid Baja interface allow some rotational motion, but restrict overall travel laterally. The concept rendering from SolidWorks® is in Figure 32.

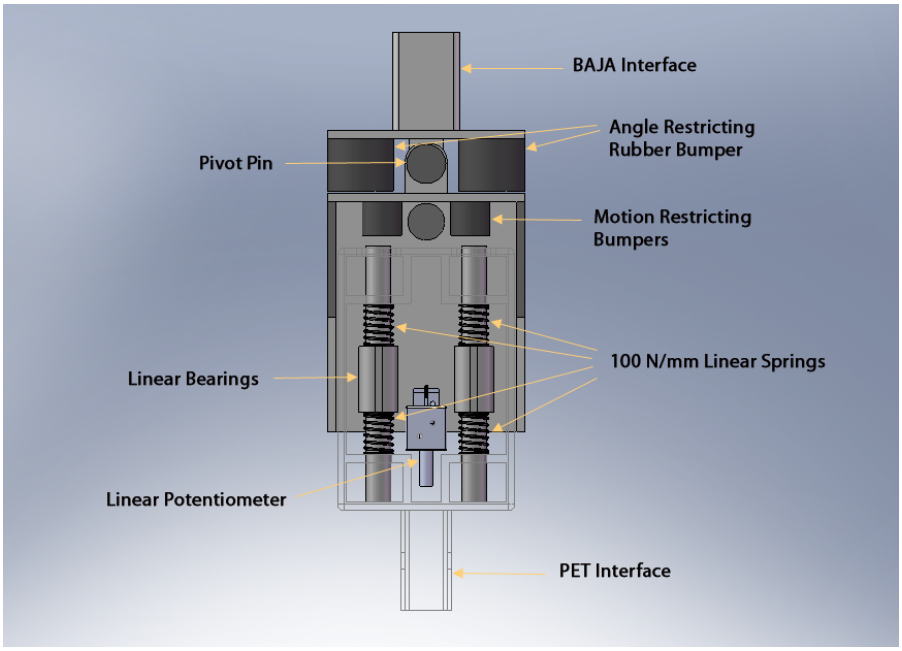

Figure 32: Push plate concept diagram used to implement the force control strategy

Figure 33 is the push plate concept designed in SolidWorks® on the left and the actual push plate on the right. The two plates are painted different colours to signify that they are separate. In between the plates are two guide shafts with one side attached to the yellow plate and the other to the green and are fixed by the bolts seen the on the top. Also inside in are two coil springs around the guide shafts for suspension. To measure the force between the two plates motion is a linear potentiometer which is calibrated and connect to the CompacRIO.

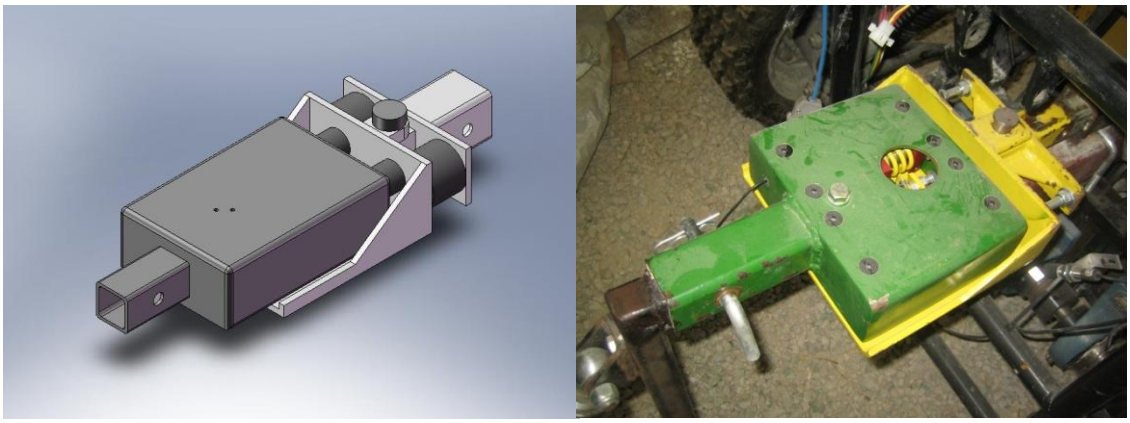

Figure 33: Push plate 3-D CAD model on the left, and the final system installed in the scaled prototype on the right

5.1.4 Data acquisition and sensory

The acquisition and instrumentation equipment for the field test apparatus is similar to the laboratory apparatus, but requires more sensors and more sophistication with the programming to test the ADD concept. For instance, the three optical and fuel flow sensors return a negative-positive-negative (NPN) pulse to the cRIO which requires a software timer for pulse width and conversion to frequency or RPM. The overall system, inputs and outputs, set and process variables for the PID controller differ from the lab test bench. Additionally, the system response is different from the lab setup and needed new programming and PID tuning. Relay circuits had to be made so the low power cRIO output could communicate with the high power DC/DC controller seen in Figure 34.

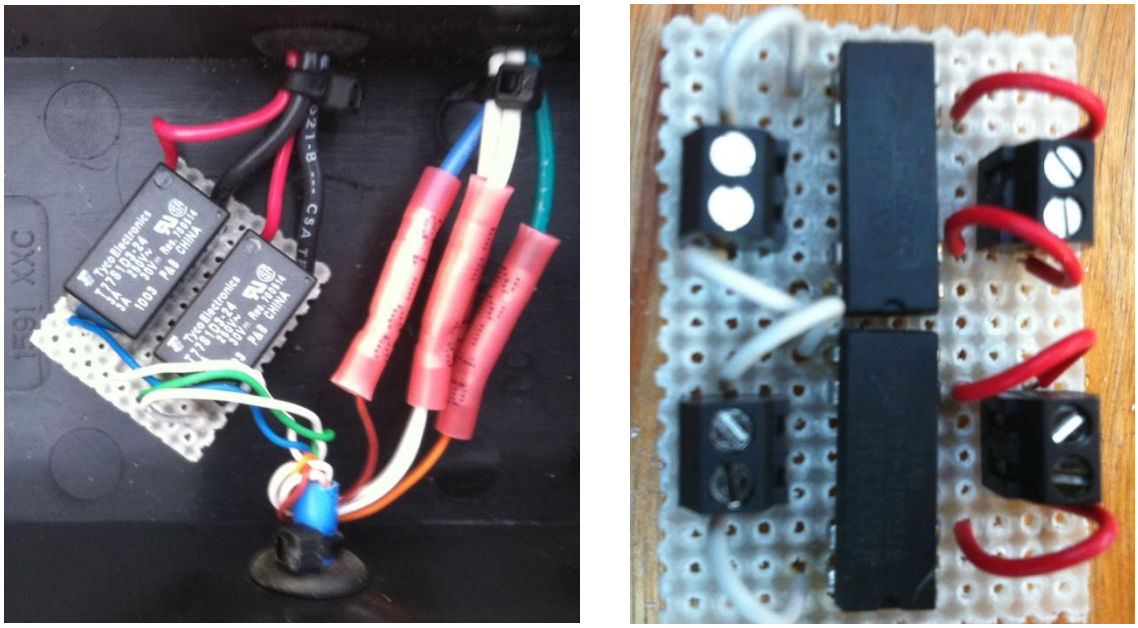

Figure 34: Relay circuits built to mediate between the low voltage NI CompactRIO and the high voltage DC/DC motor controller

Figure 35 shows the top of the back side, above the clutch and engine, of the Baja where there is the CompacRIO, the battery pack support and the voltage distribution terminals for exciting sensors.

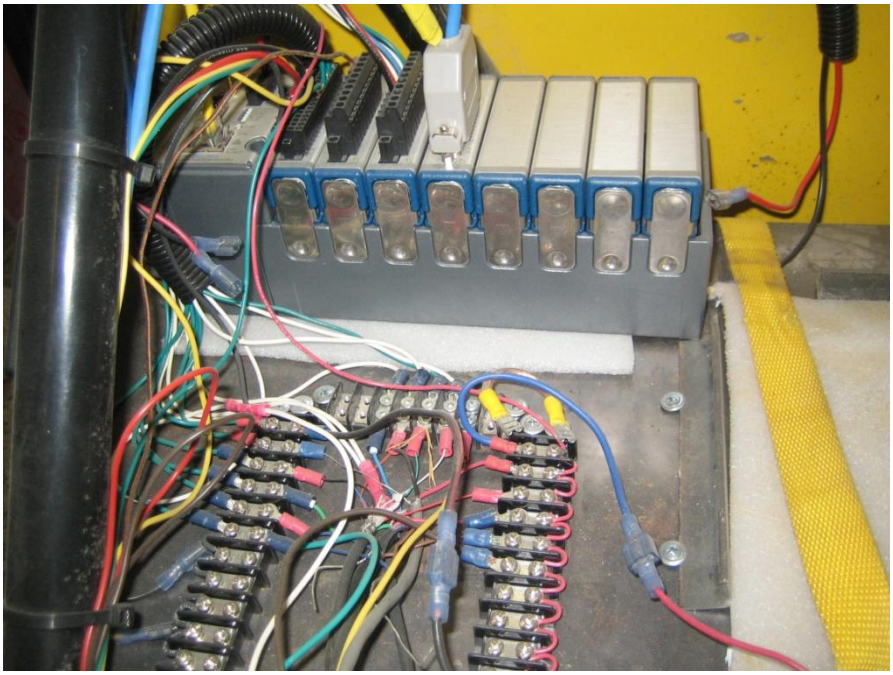

Figure 35: NI CompacRIO and voltage terminal interface on the towing vehicle

5.2 Field test results of scaled prototype

On a stretch of flat and straight road three runs of three scenarios are tested. In each case, the driver accelerates to top speed for a period, then brakes until almost full stop, and then repeats this cycle four times. First, three runs of the Baja vehicle by itself as a baseline is presented in Figure 36. Second, three runs with the ADD attached at different proportional gains in the PID controller to determine the effects of the variance on energy contribution and can be seen in Figure 37. Finally, three runs with the ADD and a trailer attached with two 15.87 kg weights over the trailer axle, again with different proportional gains and can be seen in Figure 38.

5.2.1 Baja vehicle only test results

In the three runs of only the Baja vehicle, we see variance in the velocity by the vehicle record. This may be a factor of wind conditions as drag increases exponentially with air velocity, as seen in Equation 3.1.1-2. In the simulation in Section 3.3, it is seen that the first kilometer increase in velocity lost roughly 0.04067 N-m of torque to drag forces where at top speed the final kilometer increase cost almost 1.220 N-m of torque.

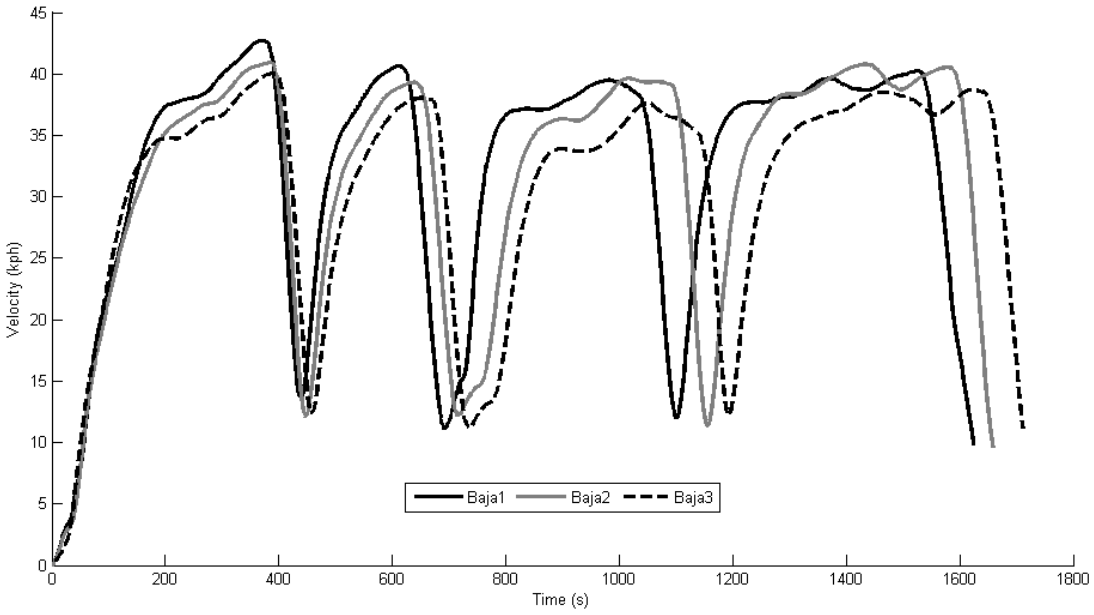

Figure 36: Three runs on flat pavement of Baja vehicle without the ADD and trailer showing vehicle velocity over time during acceleration and deceleration cycles

The top speed of the Baja in its fastest run, Baja1, is 42.9 km/hr and a trial time of 162.4 seconds or 2 minutes and 42.4 seconds. The second run also came second in top

speed at 41.2 km/hr and a trial time 165.8 seconds or 2 minutes and 45.8 seconds. The slowest run, Baja3, had a top speed of 40.2 km/hr and a trial time of 171.1 seconds or 2 minutes and 51.1 seconds. The results are tabulated in Table 15.

Table 15: Trial performance of the Baja comparing maximum velocity, acceleration and trial time

Run	Baja1	Baja2	Baja3
$\mathbf{V_{max}}$	42.9 m/s	41.2 m/s	40.2 m/s
$\mathbf{A_{max}}$	1.63 m/s^2	1.40 m/s^2	1.20 m/s^2
Trail time	02:42.4 min	02:45.8 min	02:51.1 min

5.2.2 PHEV combination: vehicle and add

In the three runs for the Baja with ADD connected, there was again a staggering in the velocities. However, aside from wind affecting drag forces, the ADD contribution is also varied by modifying the proportional gain to the PID controller.

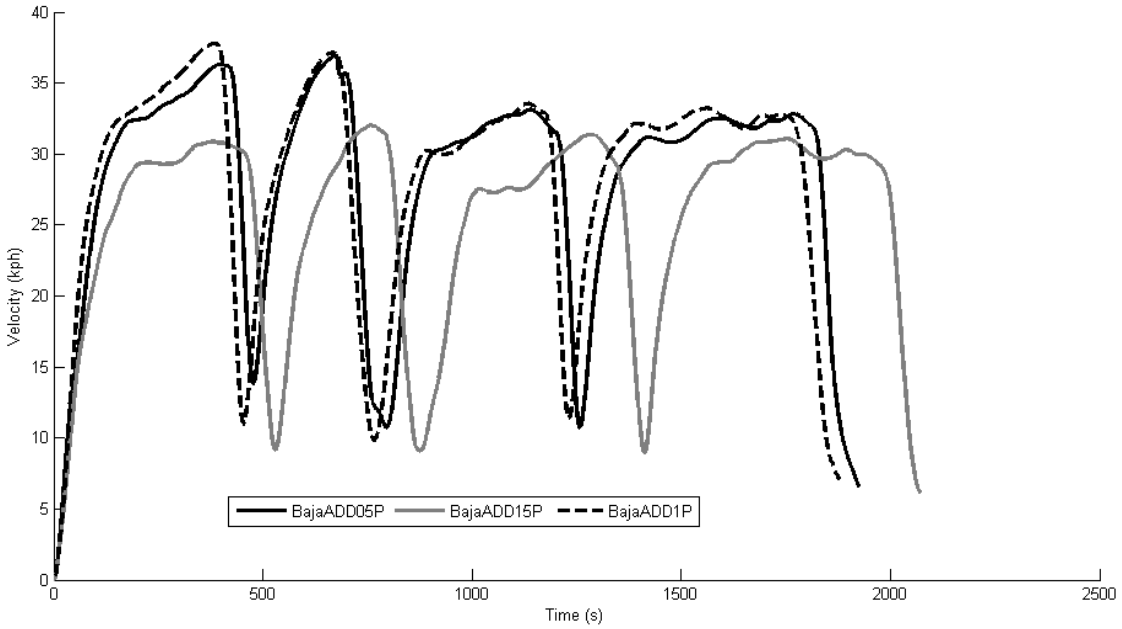

Figure 37: Three runs on flat pavement of Baja towing vehicle with ADD system going through repeated acceleration and declaration with the push plate feedback control system activated while changing the PID controller gain settings to determine performance affects.

Figure 37 is the velocity of the three runs of the Baja vehicle with the ADD attached with the proportional gains set at 0.5, 1.0, and 1.5 denoted by BajaADD05P, BajaADD1P and BajaADD15P, respectively. The difference between runs BajaADD05P and BajaADD1P seems to be slight. However, there is a definite difference in the top speed and acceleration of each cycle.

Table 16: Trial performance of the Baja and ADD system attached comparing maximum velocity, acceleration and trial time

Run	BajaADD05P	BajaADD1P	BajaADD15P
Vmax	37.2 m/s	37.9 m/s	32.2 m/s
Amax	1.07 m/s^2	1.28 m/s^2	0.98 m/s^2
Trail time	03:12.4 min	03:07.6 min	03:27.0 min

BajaADD1P had the highest top speed at 37.9 km/hr and steepest acceleration for every cycle with a trial time of 187.6 second or 3 minutes and 7.6 seconds. Close to this is the BajaADD05P with a top speed of 37.2 km/hr with a trial time of 192.4 seconds or 3 minutes and 12.4 seconds. It should be noted that the top speed in this case is on the second hump of the driving cycle, possible evidence of a wind factor. The BajaADD15P run is obviously the slowest with a top speed of only 32.2 km/hr and a trial time of 207.0 seconds or 3 minutes and 27.0 seconds. This case did not achieve the performance of the other two possibly due to the aggressive proportional gain because the activation of the ADD torque is based on the displacement incurred by the weight at the hitch. If the ADD is closing that displacement too fast it no longer contributes torque. Also, if the gain is high enough to saturate the signal of the PID controller and subsequent available voltage to contribute any torque to the system.

5.2.3 Towing vehicle configuration

The three runs with configuration of the Baja with ADD and trailer attached show similar staggering, due to reduction in top speeds increasing the overall trial time of each driving cycle.

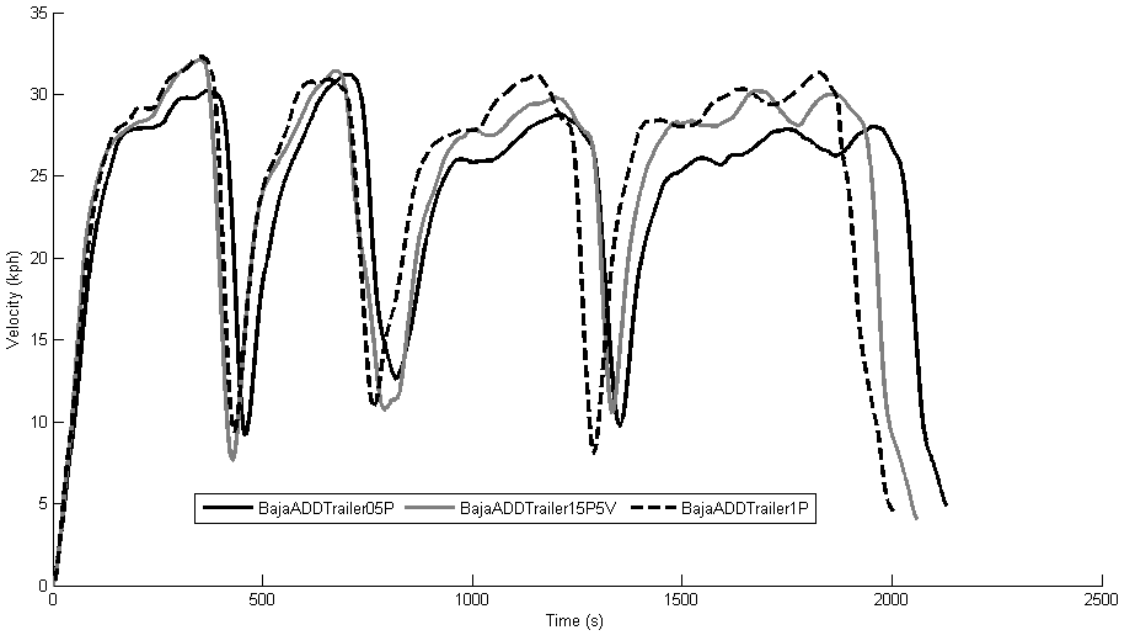

Figure 38: Three runs on flat pavement of Baja towing vehicle with ADD and trailer attached going through repeated acceleration and declaration with the push plate feedback control system activated

Figure 38 is the three runs of the Baja vehicle with the ADD and weighted trailer attached operating as a vehicle in tow mode. First is the BajaADDTrailer1P with the highest top speed of 32.4 km/hr and the most aggressive acceleration and a trial time of

200.3 seconds or 3 minutes and 20.3 seconds. A close second, is the BajaADDTrailer15P5V at a top speed of 32.0 km/hr and a trial time of 205.9 seconds or 3 minutes and 25.9 seconds. The 5 V in the title of the run denotes the increase of the analog signal, from the computer to the controller, from 4 volts to 5 volts in an attempt to raise the saturation point. The analog output is limited to 4 volts to increase stability in the system because many of the initial runs were erratic. The effect of this increase is significant as this run competes for the best performance as seen in Table 17.

Table 17: Trial performance of the Baja with the ADD system and trailer attached comparing maximum velocity, acceleration and trial time

Run	BajaADDTrailer05P	BajaADDTrailer1P	BajaADDTrailer15P5V
Vmax	31.4 m/s	32.4 m/s	32.0 m/s
Amax	0.81 m/s^2	0.98 m/s^2	0.99 m/s^2
Trail Time	03:32.8 min	03:20.3 min	03:25.9 min

Finally, the BajaADDTrailer05P with a top speed of 31.4 km/hr, occurring in the second hump of the driving cycle, and a trial time of 212.8 seconds or 3 minutes and 32.8 seconds. The proportional gain of 1.0 for the PID controller seems to be most appropriate for compensation of the load. With the addition of the trailer the ADD seems to no longer saturate and the displacement seen in the push plate remains active for the torque contribution.

5.2.4 Configuration comparison

The best performing run from each configuration is selected. The staggering in the velocity is profound between the Baja alone and it with attachments shown here in Figure 39.

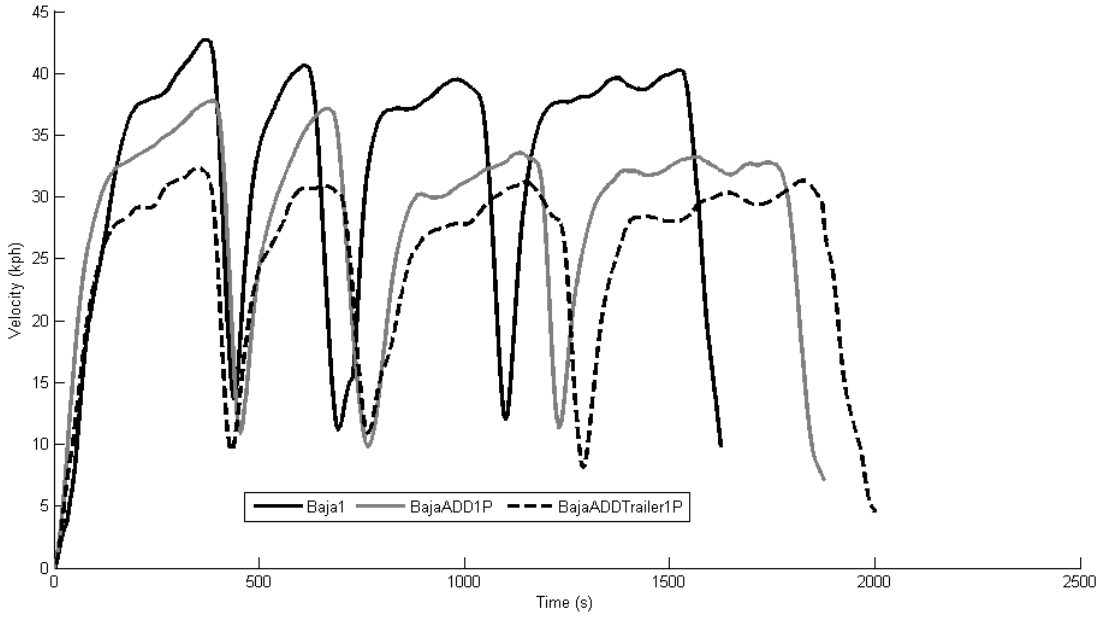

Figure 39: The best run of each configuration, Baja, Baja-ADD, and Baja-ADD-Trailer compared going through repeated acceleration and declaration with the push plate feedback control system activated

The differences in top speed are shown by the pronouncement of staggering seen in Figure 39. Revealing, on a velocity basis, the ADD is not able to reconcile the weight of the ADD or trailer entirely. The additional weight of either the ADD or trailer has an

effect on top speed and maximum acceleration. The top speed of the Baja vehicle alone is 43 km/hr where with the ADD addition is 38 km/hr and with the ADD and trailer only at 32 km/hr, and for acceleration the same order of vehicle configurations appear 1.63 m/s^2, 1.28 m/s^2, and 0.98 m/s^2 respectively.

Table 18: Trial performance of the Baja with the ADD system and trailer attached comparing maximum velocity, acceleration and trial time

Run	Baja1	BajaADD1P	BajaADDTrailer1P
Vmax	42.9 m/s	37.9 m/s	32.4 m/s
Amax	1.63 m/s^2	1.28 m/s^2	0.98 m/s^2
Trail Time	02:42.4 min	03:07.6 min	03:20.3 min

The ADD contributes to velocity and acceleration of the overall vehicle and trailer set shown significantly on fuel consumption by weight basis in Table 19 shows a gain of 23.6% savings in fuel consumption per pound with the ADD attached to the Baja and 51.1% with the ADD and trailer attached. The difference between them is 27.5%.

Table 19: Comparative fuel usage data of the best runs, Baja, Baja-ADD and Baja-ADD-Trailer going through the driving cycle with the push plate feedback control system activated

	Baja1	**BajaADD1P**	**BajaADDTrailer1P**
Fuel consumed by run	360.7 ml	375.6 ml	400.8 ml
Fuel consumed by weight	1.235 ml/kg	0.9480 ml/kg	0.5952 ml/kg
Difference		23.6%	51.1%
Comparative Difference			27.5%

5.3 Discussion of results

The laboratory test bench validated the design of the push plate. It is shown that this device could be implemented as a force input to an electrical hybrid addition. The software developed is able to reasonably follow the push/pull forces of the simulated device of a towing vehicle. It is shown that this method of springs and a linear potentiometer could be adequate for sensing the towing forces of a trailer on a vehicle.

When the proportional gain is varied between 0.5 and 1.5 there are significant performance differences. In the Baja-ADD configuration, the 1.0 proportional gain performed the best. Again for the Baja-ADD-Trailer the 1.0 proportional gain excelled while expectantly the 1.5 followed and the 0.5 performed the poorest.

Table 20: Percentage energy savings comparison between the Baja alone to the Baja with ADD system and Baja with ADD system and trailer attached.

	Baja + ADD	**Baja + ADD + Trailer**
Model Analysis	27.2 %	57.5 %
Field Test	23.6 %	51.1 %
% Difference	3.6 %	6.4 %

After all the measurements and calculations the spreadsheet analysis revealed a 27.2% reduction in vehicle torque with the ADD and 57.5% with the ADD and Trailer attached on a per pound basis. The field performance through the driving cycle is the best for the Baja vehicle alone followed by the Baja-ADD then the Baja-ADD-Trailer. The field results confirmed the system model analysis results with 23.6% for the addition of the ADD and 51.1% for the ADD and trailer configuration. The Baja alone retained the highest speed followed by the ADD and ADD and trailer attached. The percentage comparison is in Table 20.

6 Conclusion and recommendations

6.1 Conclusions

Today's modes of transport rely on the burning of fossil fuels with harmful exhaust emissions. The ADD can provide a novel electrification of fossil fuel vehicles to reduce these emissions on a vehicle with or without towing a trailer. Field testing for a vehicle in tow, revealed that during the ADD tests, torque contributions are positive and validate the concept, but still short of what is expected. This may have been caused by any number of reasons, especially wind factors, not in the model, seemed to play a significant role as can be seen in Section 5.2.1 with the Baja alone a margin of almost 10%. Regardless, the ADD system is able to compensate for over 50% of the trailer load. This is notable considering the ADD and trailer with weights is about three quarters the weight of the Baja with a driver. The next step will be to compensate for the trailer load. This may require the substitution of the push plate as it necessarily needs that pulling force of the trailer. A larger motor and battery pack could be designed to provide higher torque and energy contributions, as well regenerative braking could contribute significantly to the overall fuel consumption of the vehicle.

6.2 Future optimization of design

During this project issues arose with the concept of the push plate device and ADD system. The current push plate design relies on the displacement of two springs and bearings with a single linear potentiometer to determine the force magnitude. This is unreliable because the spring rates are assumed to be linear and linear bearings can bind causing friction, not translated as displacement, which can be problematic when measuring displacement only with all the bumps and articulation in the context of typical road conditions. Compounding this problem is that this form of the concept has suspension with a lateral component that influences the push plate on every bump or frame displacement, which may have contributed to the ADD performing poorer than the ADD with a trailer attached. The control strategy did have a dampened response to filter out random push plate displacement of significant magnitude belaying any inappropriate input of torque.

Additionally, considering the ADD is an articulating axle behind the vehicle so when torque is applied it is almost never coincident with the COG of the vehicle causing varying degrees of instability. The more effective or permanent solution would be to orientate the spring and damper to an incident vector perpendicular to the PP or force sensing device. A possible outcome is to have a dual wheel design with double wish bone control arms and opposing suspension which is commonly used in most production vehicles and is present in the towing vehicle of this project.

The purpose of the push plate is to quantify the magnitude of force subjected to the towing vehicle from a trailer or from the ADD alone. This can be determined by several methods, however, the three that are relevant are "through the road", strain on the adjoining rigid member or a combination of the two. "Through the road", in this case, is where the control system instead of sensing force or displacement will sense the rpm of the wheel on the ADD subjected by traction on a road surface then referencing a predetermined value of contributing torque. Second would be to substitute the push plate with a load cell integrated in the rigid connection between the towing vehicle and trailer determining force more directly through strain. Advantages would be fewer parts, meaning less risk of failure or malfunction such as binding, as well load cells are widely trusted in many industries and are reliable devices in general and especially for this type of measurement. Third, a possible ideal solution would be a combination of both: the ADD control system would sense both the subjected force and rpm to determine torque contribution. Where either system could be employed depending of the circumstance. For example, without a trailer it would be more appropriate to use "through the road" as it does not require a towing force. Alternately, the load cell would be more appropriate in the condition of the trailer being attached where towing forces are applied.

Further advancing the concept would be to implement regenerative braking. Allowing the ADD to siphon charge from the towing vehicle in a "through the road" fashion, choosing ideal times like extended highway driving and more importantly in actual braking conditions where the trailer contributes a significant force. The ADD control strategy would dictate the EM to recover current from the rotation providing a braking

force requiring a different battery pack as the gel cell batteries used are limiting in their acceptance of charge. Specified charging is with minimal current and in this project were charged only with an external trickle charger submitting less than 2 A of current. Future iterations would benefit from simplified compact onboard integrated circuitry and charge control allowing generic home outlet charging and regenerative braking. Regenerative braking requires high current acceptance which would require some kind of large capacitor to compensate and battery packs, possibly of a type of NiMH or LI-ion, which are able to sustain higher current draw. Batteries of this type would provide better performance and longer ranges with significantly higher power to ratios amongst other advantages.

Finally, a full size vehicle would be more appropriate as opposed to the one used in this project where there were many obstacles surrounding the use of the SAE Baja for this application. A full size production vehicle will already have many sensors and valuable data accessible through a CANBUS system saving in instrumentation. Also, for a production vehicle many specifications and ratings would be available compared to the student designed custom SAE Baja where these values would have to be measured or estimated for simulation, as can be seen in Appendix C. Ultimately, only in the "real world" scenario of a full size towing vehicle would the actual form, performance and benefit of the ADD system be quantified accurately.

References

[1] Ministry of Transport, "Transportation in Canada 2000: Annual Report," Minister of Public Works and Government Services, Ottawa, 2000.

[2] Ministry of Transport, "Transportation in Canada 2001: Annual Report," Ministry of Public Works and Government Services, Ottawa, 2001.

[3] Ministry of Transport, "Transportation in Canada 2002: Annual Report," Ministry of Public Works and Government Services, Ottawa, 2002.

[4] Ministry of Transport, "Transportation in Canada 2003: Annual Report," Ministry of Public Works and Government Services, Ottawa, 2003.

[5] Ministry of Transport, "Transportation in Canada 2004: Annual Report," Mintry of Public

Works and Government Services, Ottawa, 2004.

[6] Ministry of Transport, "Transportation in Canada 2005: Annual Report," Ministry of Public Works and Government Services, Ottawa, 2005.

[7] Ministry of Transport, "Transportation in Canada 2006: Annual Report," Ministry of Public Works and Government Services, Ottawa, 2006.

[8] Ministry of Transport, "Transportation in Canada 2007: An Overview," Ministry of Public Works and Government Services, Ottawa, 2007.

[9] Ministry of Transport, "Transportation in Canada 2008: An Overview," Ministry of Public Works and Government Services, Ottawa, 2008.

[10] Ministry of Transport, "Transportation in Canada 2009: An Overview," Ministry of Public

Works and Government Services, Ottawa, 2009.

[11] D. Sawicz, "Hobby Servo Fundamentals," Princeton University, Princeton, 2002.

[12] T. C. a. W. Summers, American Electricans' Handbook, Eleventh Edition, New York: McGraw-Hill, Inc., 1987.

[13] P. V. d. Bossche, "File:Hybridpeak.png," 2009. [Online]. Available: http://commons.wikimedia.org/wiki/File:Hybridpeak.png. [Accessed 2012].

[14] P. V. d. Bossche, "File:Hybridpar.png," 2009. [Online]. Available: http://en.wikipedia.org/wiki/File:Hybridpar.png. [Accessed 2012].

[15] P. V. d. Bossche, "File:Hybridcombined.png," 2009. [Online]. Available: http://en.wikipedia.org/wiki/File:Hybridcombined.png. [Accessed 2012].

[16] C. S. Siskind, Electrical Control Systems in Industry, New York: McGraw-Hill, Inc., 1963.

[17] H. Sun, J.-h. Jiang and X. Wang, "Torque control strategy for a parallel hydraulic hybrid vehicle," vol. 46, no. 0022-4898, 2009.

[18] Z. e. a. Shupeng, "Control Strategy and Simulation Analysis of Hybrid Electric Vehicles," 2007.

[19] S. J. Boyd, "Hybrid Electric Vehicle Control Strategy Based on Power Loss Calculations," Virginia Polytechnic Institute and State University, Blacksburg, 2006.

[20] J. M. Morbitzer, "High-Level Modeling, Supervisory Control Strategy Development, and Validation for a Proposed Power-Split Hybrid-Electric Vehicle Design," Ohio State University, Columbus, 2005.

[21] N. M. Picot, "A Strategy to Blend Series and Parellel Modes of Operation in a Series-Parellel 2-by-2 Hybrid Diesel/Electric Vehicle," University of Akron, Akron, 2007.

[22] T. D. Gillespie, Fundamentals of Vehicle Dynamics, Warrendale: Society of Automotive Engineers Inc., 1992.

[23] Perm Motor GMBH, "Condensed Power for Mobile Applications," Perm Motor GMBH, Kesslerstrasse, 2009.

[24] Akron, "Absolute Top Speed of Competition Ready Car," 02 July 2012. [Online]. Available: http://forums.bajasae.net/forum/absolute-top-speed-of-competition-ready-car_topic1037.html. [Accessed 2012].

[25] Jack's Small Engines and Generator Service, LLC, "Briggs & Stratton 10 Hp Intek Engine," Jack's Small Engines and Generator Service, LLC, 2012. [Online]. Available:

http://www.jackssmallengines.com/bs10intekpro.html. [Accessed 2012].

[26] S. J. Chapman, Electric Machinery Fundamentals, New York: McGraw-Hill, 2005.

[27] J. B. Heywood, Internal Combustion Engine Fundamentals, New York: McGraw-Hill, 1988.

[28] J. Taxis, "2013 Bearcats Baja Braking System," University of Cincinnati/SAE International, Cincinnati, 2013.

[29] University of Utah, "Engine Data," University of Utah, 2005. [Online]. Available: http://www.mech.utah.edu/senior_design/05/index.php/MiniBaja2/Enginedata. [Accessed 2012].

Appendix A: DAQ software

The following is the LabVIEW program developed to run the field testing system. In order to control the ADD concept and to implement the PID control strategy for the field test. The program has many sub level programs and conditional subsets, as shown in Figures A.1 and A.2.

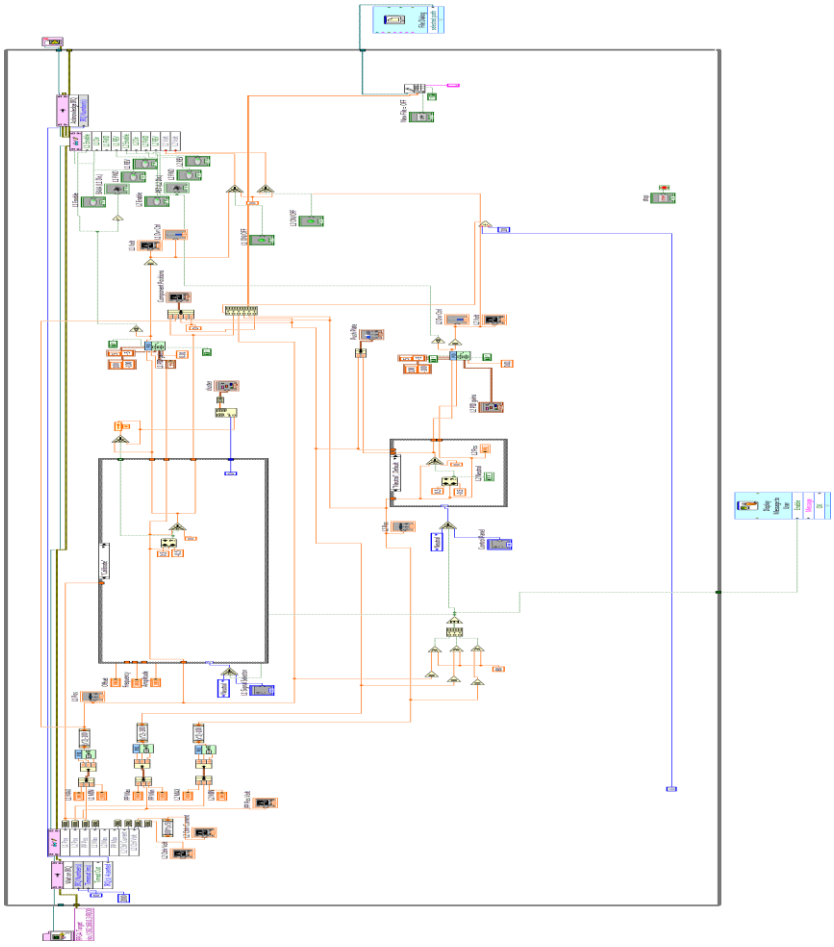

Figure 40: Control model for the test vehicle with the ADD

This is the interface developed for human control and real-time following of what is happening with the system(s) involved.

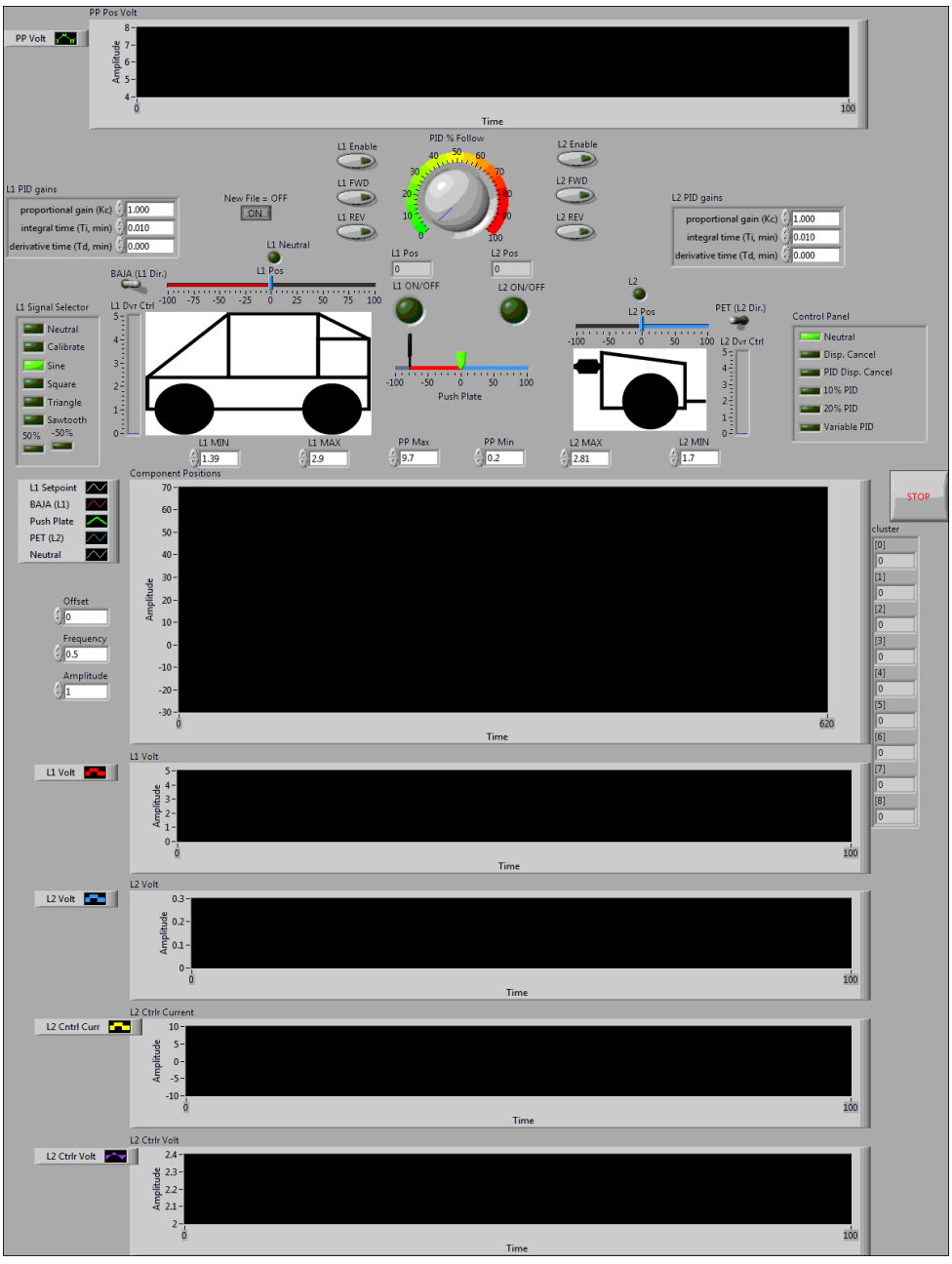

Figure 41: DAQ system interface for bench lab scale system

Appendix B: Matlab® code

The following the Matlab® program is one of the many routines developed to analyze and build the field test data discussed in Section 5.2.

```
clc
clear all
close all
hold all
set(0,'defaulttextinterpreter','tex');

% Adjustable Variables
LineSize=2.5;
delimiter='\t';
DataStart=0;
Row=1;
Col=7;
Fs=100;
SampleTime=1/Fs;
TimeStart=0;
TimeStop=7000;

% Set axes properties
set(gca, 'ColorOrder', [0 0 0; 0.5 0.5 0.5]); % just black and grey
set(gca, 'LineStyleOrder', {'-', '--', ':', '-.'}); % different line styles

% Get Files and Names
files = dir('*.txt');
filenames = {files.name};
c=[1:length(files)];
tt=[1:length(files)];

% Load Data
for i=1:length(files)
    eval(['load ' files(i).name ' -ascii']);
    filename = files(i).name;
    d=dlmread(filename);
    T{i}=d(:,2);

    f{i}=d(:,4);
    k=0;
    for k=1:length(f{i}(:,1))
       if (k+1)<length(f{i}(:,1))&&f{i}(k,1)~=f{i}(k+1,1)
           c(i)=c(i)+1; % Pulses
       end
    end
```

```
fl(1,i)=c(i)/1547; % Litres consumed
fl(2,1)=fl(1,i)/713;  % Litres per Pound Weight
fl(2,2)=fl(1,i)/(713+220);
fl(2,3)=fl(1,i)/(713+220+525);
fl(3,2)=(abs(fl(2,2)-fl(2,1))/fl(2,1))*100;
fl(3,3)=(abs(fl(2,3)-fl(2,1))/fl(2,1))*100;

tmax(i)=SampleTime*(length(f{i}));
fs{1,i}=10000*sum(1/(1547*f{i}));
fs{2,1}=fs{1,i}/713;
fs{2,2}=fs{1,i}/(713+220);
fs{2,3}=fs{1,i}/(713+220+525);
fs{3,i}=fs{1,i}/length(f{i});
v{i}=d(:,7);
r{i}=d(:,8);
ax{i}=d(:,9);
pv{i}=d(:,12);
ps{i}=d(:,13);
pc{i}=d(:,14);
% data{i}=dlmread(filename);
[B,A]=butter(2,0.03);
Tf{i}=filter(B,A,T{i});
ff{i}=filter(B,A,f{i});
fsf{i}=sum(1/(1547*ff{i}));
vf{i}=filter(B,A,v{i});
vs(1,i)=sum(vf{i});
rf{i}=filter(B,A,r{i});
axf{i}=filter(B,A,ax{i});
vms{i}=vf{i}*1000/3600;
vmax(i)=max(vf{i});

tf{i}=5*((9*10^(-7))*rf{i}+(0.0046*rf{i})+7.5989);
ta{i}=(0.1434*axf{i}+0.082)/8;

j=0;
for j=1:length(tf{i}(:,1))
   if (j+1)<length(vms{i}(:,1))&&vms{i}(j,1)<vms{i}(j+1,1)
        a{i}(j,1)=(vms{i}(j+1,1)-vms{i}(j,1))/0.1; % acceleration
   end
    if (j+1)<length(tf{i}(:,1))%&&tf{i}(j,1)<=tf{i}(j+1,1)
       tt(i)=tt(i)+tf{i}(j,1);
   end
end

amax(i)=max(a{i});
tfmax(i)=max(tf{i})
tamax(i)=max(ta{i})

ts(1,i)=sum(tt(i));
ts(2,1)=ts(1,i)/713;
ts(2,2)=ts(1,i)/(713+220);
ts(2,3)=ts(1,i)/(713+220+525);
ts(3,2)=(abs(ts(2,2)-ts(2,1))/ts(2,1))*100;
ts(3,3)=(abs(ts(2,3)-ts(2,1))/ts(2,1))*100;
```

```
    af{i}=8*filter(B,A,ax{i});
    atf{i}=((9*10^(-7))*af{i}+(0.0046*af{i})+7.5989);
    pvf{i}=filter(B,A,pv{i});
    psf{i}=filter(B,A,ps{i});
    pcf{i}=filter(B,A,pc{i});
    [pathstr,name,ext] = fileparts(filename);
    %
[time,data]=DataWindow(filename,delimiter,Row,Col,SampleTime,DataStart,TimeSt
art,TimeStop);
    [x{i},y{i}]=max(ff{i});
    ys{i}=y{i}*SampleTime;
    % t=t(find(t>=TimeStart&t<=TimeStop));
    h=plot(tf{i},'linewidth',LineSize,'erasemode','background');
%     plot(rf{i},'linewidth',LineSize,'erasemode','background');
    % title('');
    % Peak{i}=num2str(sprintf(', max@ %.2f', x{i}));
    l{i}=name;%strcat(name, Peak{i});
end
vs(2,2)=(abs(vs(1,2)-vs(1,1))/vs(1,1))*100;
vs(2,3)=(abs(vs(1,3)-vs(1,1))/vs(1,1))*100;

% Plot Settings
set(gcf,'position',[680 407 1101 571]);
legend(l{:},'location','best','orientation','horizontal');
xlabel('Time (s x 10^-^1)');
ylabel('Velocity (km/hr)');
return

for k=1:length(files)
    subplot(211),plot(vf{k},'linewidth',LineSize,'erasemode','background');
    hold all
end

for k=1:length(files)
    subplot(212),plot(Tf{k});
    hold all
end


[Throttle,Torque,Fuel_lph,Fuel_lps,Fuel_V,VarName6,Speed_kph,Engine_rpm,Axle_
rpm,VarName10,VarName11,PETvolt,PETsoc,PETcurrent]=B1('B1_Data',1,10000);
plot(Torque);
grid on
hold on
```

Appendix C: Simulink® model

Simulink® was used in an attempt to develop a more sophisticated simulation of the overall ADD system. However, the model could not always yield stable and realistic results because the details required to define some of the required physical properties remained largely uncharacterized and there estimate was outside the scope of this project. As an example, Simulink® required the inertia of the belt clutch and spindle system which is a complex system of moving components. Figures C.1 to C.3 shows various examples of the model.

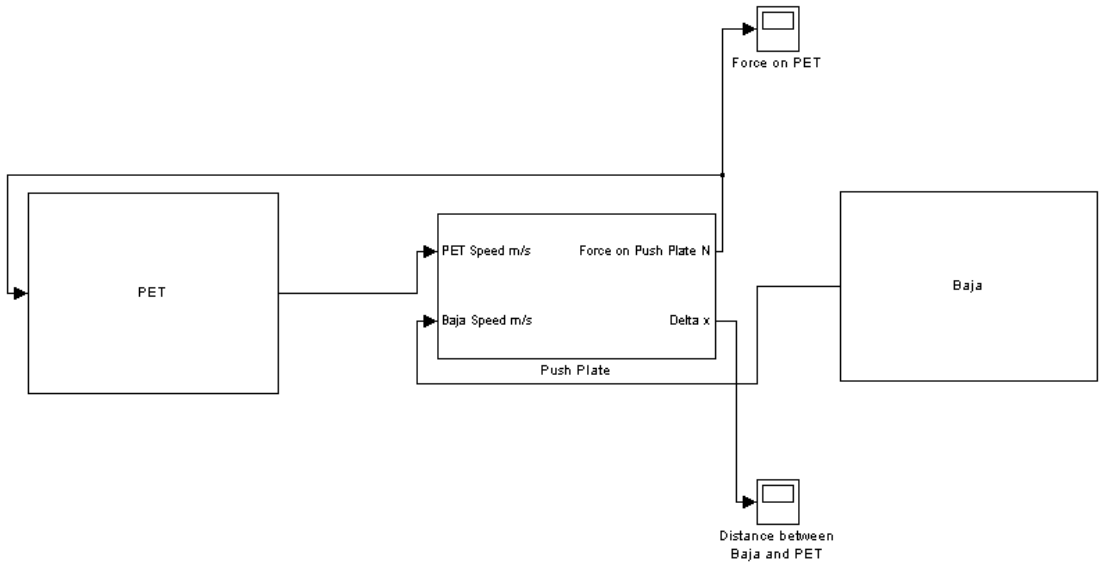

Figure 42: The overall Baja, ADD (PET), and trailer system

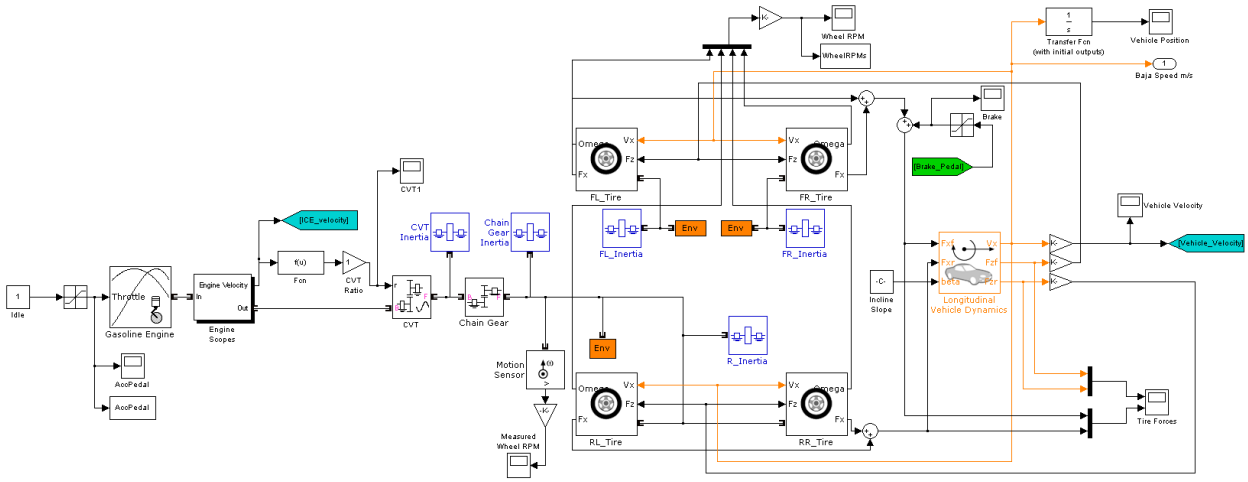

Figure 43: The SAE Baja vehicle model

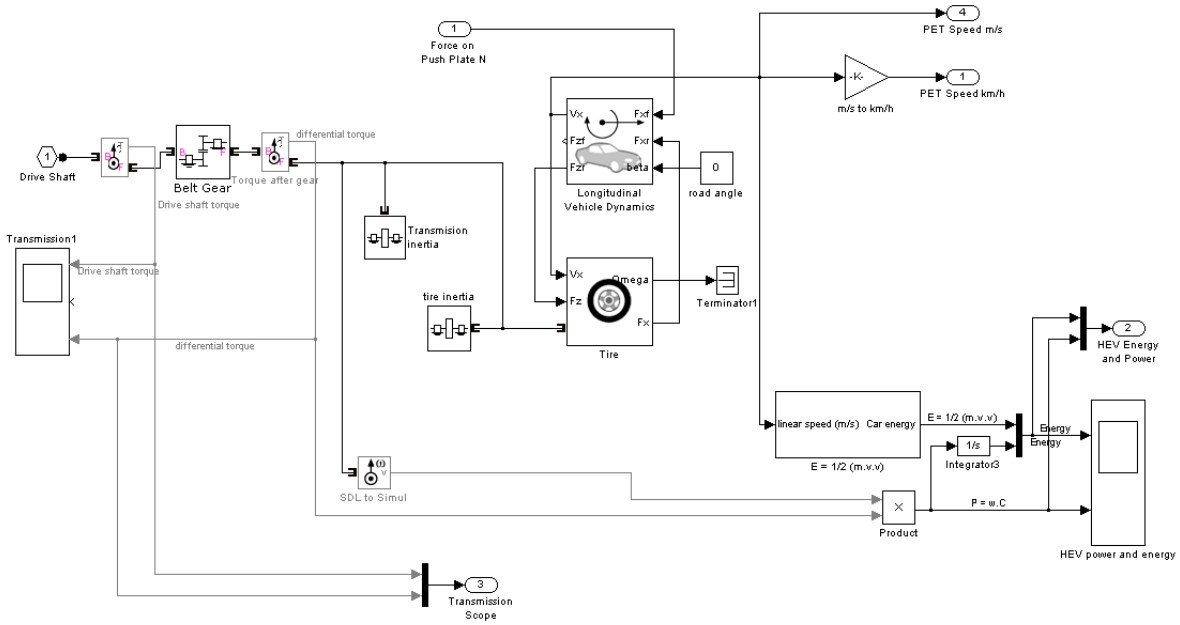

Figure 44: The ADD concept model